Syst. Biol. 55(2):208–227, 2006

ISSN: 1063-5157 print / 1076-836X online
DOI: 10.1080/10635150500481317

Molecular Phylogenetic Analyses Indicate Multiple Independent Emergences of Parasitism in Myzostomida (Protostomia)

DEBORAH LANTERBECQ,[1] GREG W. ROUSE,[2] MICHEL C. MILINKOVITCH,[3] AND IGOR EECKHAUT[1]

[1]*Marine Biology Laboratory, University of Mons-Hainaut (UMH), 6 Avenue du champ de Mars, Life Sciences building, 7000 Mons, Belgium; E-mail: deborah.lanterbecq@umh.ac.be (D.L.); igor.eeckhaut@umh.ac.be (I.E.)*
[2]*South Australian Museum, Adelaide, Australia; School of Earth and Environmental Sciences, University of Adelaide, SA 5000, Australia*
[3]*Unit of Evolutionary Genetics (CP 300), Free University of Brussels (ULB), Institute of Molecular Biology and Medicine, 6041 Gosselies, Belgium*

Abstract.—The fossil record indicates that Myzostomida, an enigmatic group of marine worms, traditionally considered as annelids, have exhibited a symbiotic relationship with echinoderms, especially crinoids, for nearly 350 million years. All known extant myzostomids are associated with echinoderms and infest their integument, gonads, celom, or digestive system. Using nuclear (18S rDNA) and mitochondrial (16S and COI) DNA sequence data from 37 myzostomid species representing nine genera, we report here the first molecular phylogeny of the Myzostomida and investigate the evolution of their various symbiotic associations. Our analyses indicate that the two orders Proboscidea and Pharyngidea do not constitute natural groupings. Character reconstruction analyses strongly suggest that (1) the ancestor of all extant myzostomids was an ectocommensal that first infested crinoids, and then asteroids and ophiuroids, and (2) parasitism in myzostomids emerged multiple times independently. [Character evolution; commensalism; crinoids; echinoderms; molecular phylogeny; myzostomids; symbiosis.]

Myzostomids are small marine worms found in all oceans, from the intertidal to the abyssal zone. This group comprises about 170 species that are all associated with echinoderms: there exists neither free-living species nor species living symbiotically with non-echinoderm hosts (but see Grygier, 2000, for possible exceptions). Of the five extant echinoderm classes, crinoids, asteroids, and ophiuroids can be infested by myzostomids (>90% of myzostomids are associated with comatulid crinoids). Living crinoids can be informally split into two categories: stalked crinoids (about 30 genera and 95 species; Roux et al., 2002), or "sea lilies," living attached to the substratum predominantly in the oceanic bathyal zone, and comatulid crinoids (140 genera, 500 species; Messing, 1997), or "feather stars," including the stalkless (in fact, the topmost stalk segment is retained; Messing, 1997) vagile crinoid species that can be found from shallow to deep waters.

Host specificity is high as many myzostomid species are associated with a single crinoid species (Eeckhaut et al., 1998), although a few species exhibit some level of flexibility in their host associations. Another striking characteristic of the echinoderm-myzostomid symbiosis is its remarkable persistence through evolutionary times: although the myzostomid origin of marks left on Ordovician crinoids (Warn, 1974) have been questioned (Eeckhaut, 1998), unambiguous signs of myzostomid activities are present on fossil crinoids dating back to the Carboniferous (Meyer and Ausich, 1983; Brett, 1978).

The long association between echinoderms and myzostomids has promoted the evolution of a diverse array of myzostomid morphologies and symbiotic lifestyles. Indeed, although most myzostomids are ectocommensal and move on their comatulid crinoid host, many species specialize in their preferred localization on their host: the calyx (Fig. 1A), the arms (Fig. 1B), or the pinnules (Fig. 1C). These myzostomids steal food particles before they reach the host's mouth. Other myzostomid species are endoparasites of stalked or comatulid crinoids and live in the integument (where they form galls or cysts; Fig. 1D), digestive system (Fig. 1E), gonads, or celomic cavities (Fig. 1F) of their host. Although some of these forms also steal food particles from the crinoid rather than actually eating the host directly, we here refer to all of them as parasitic. Gallicolous and cysticolous myzostomids both live in shelters whose walls are made by crinoid tissues (Jangoux, 1990). In the former, the walls are hardened by crinoid ossicles that are deformed by the presence of the parasites. In the latter, the walls are either made of soft tissues or reinforced by minute skeletal plates whose formation is induced by the presence of the parasite. A minority of myzostomid species is known to parasitize the integument or digestive caeca of asteroids and the gonads or bursa of ophiuroids (Grygier, 2000).

The diversity of myzostomid morphologies is paralleled by an array of different lifestyles. In most myzostomids, the body consists of (i) a trunk of variable shape, curvature, and thickness depending upon the taxon considered (Figs. 1G–J) and (ii) an anterior introvert (also called proboscis; Fig. 1K). The trunk has a length that ranges from a few millimeters to three centimeters, and ventrally has five pairs of locomotory organs (the parapodia) and four pairs of sense organs (commonly called "lateral organs," alternating with parapodia) (Fig. 1L). Each parapodium comprises a cone with a hook-shaped chaeta distally and a basal parapodial fold (Fig. 1M). The margin of the trunk often bears cirri (Figs. 1G, I, J, L) that might act as chemosensory organs involved in the recognition of the substratum, i.e., the echinoderm-host surface (Eeckhaut and Jangoux, 1991). Some ectocommensal species have caudal processes (Fig. 1G) mimicking the pinnules of the host (Fig. 1B). Parasitic species (Fig. 1H, J) are highly modified with the reduction, or even the absence, of locomotory and sensory organs.

The heterogeneity of anatomical features observed in myzostomids obscures their phylogenetic position within Metazoa (see Eeckhaut and Lanterbecq, 2005). Because they exhibit segmentation (although incomplete),

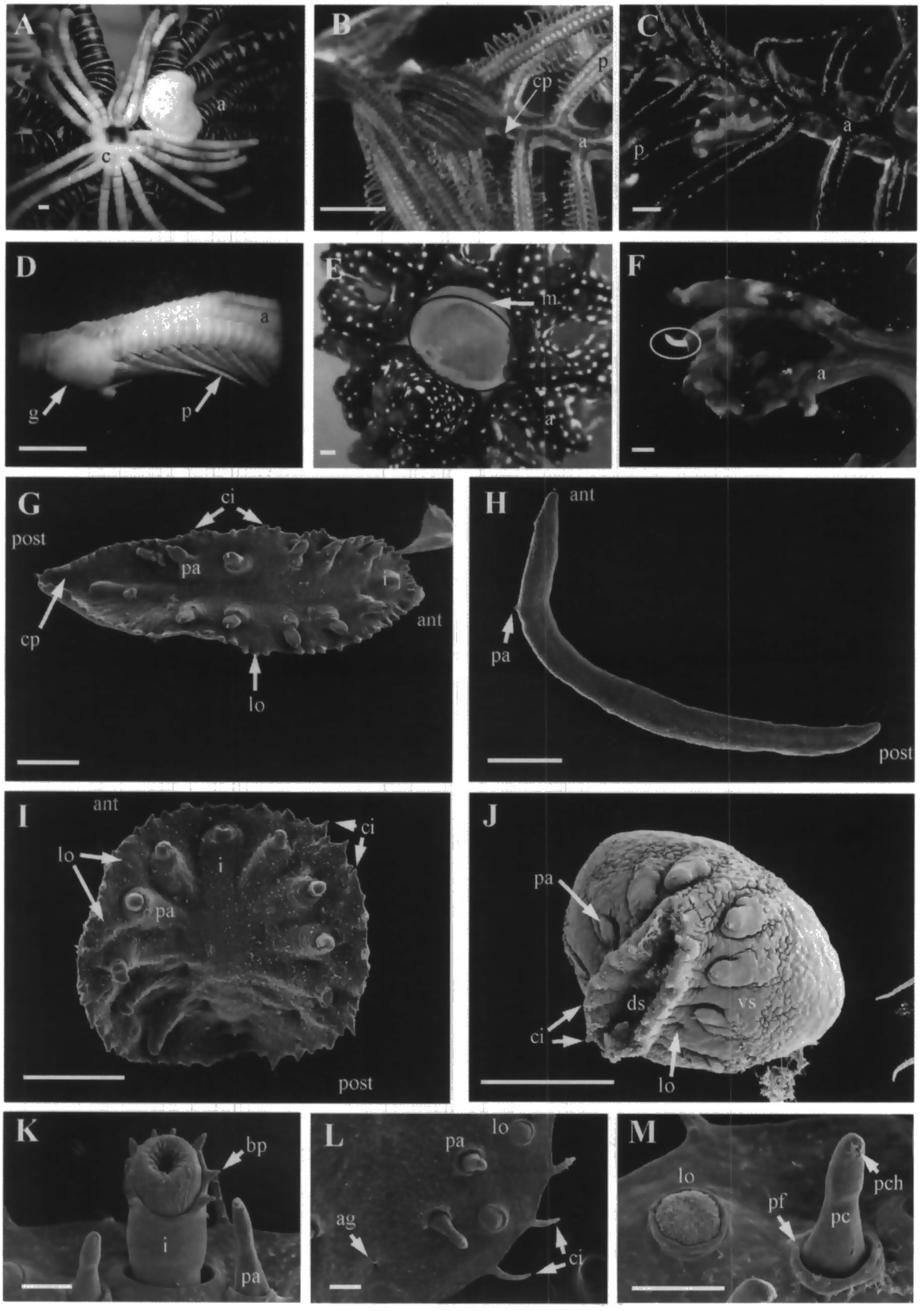

TABLE 1. Classification of extent Myzostomida (Grygier, 2000).

Class Myzostomida
- Order Proboscidea Jägersten, 1940
  - Family Myzostomatidae Beard, 1884
    - Genus *Myzostoma**
    - Genus *Notopharyngoides**
    - Genus *Hypomyzostoma**
- Order Pharyngidea Jägersten, 1940
  - Family Pulvinomyzostomatidae Jägersten, 1940
    - Genus *Pulvinomyzostomum**
  - Family Endomyzostomatidae Perrier, 1897*
    - Genus *Endomyzostoma**
    - Genus *Contramyzostoma**
    - Genus *Mycomyzostoma*
  - Family Mesomyzostomatidae Stummer-Traunfels, 1923
    - Genus *Mesomyzostoma**
  - Family Protomyzostomatidae Stummer-Traunfels, 1923
    - Genus *Protomyzostomum**
  - Family Asteromyzostomatidae Wagin, 1954
    - Genus *Asteromyzostoma**
  - Family Asteriomyzostomatidae Jägersten, 1940
    - Genus *Asteriomyzostoma*
  - Family Stelechopidae Graff, 1884
    - Genus *Stelechopus*

Genera marked with an asterisk have been used in the present study.

parapodia with chaetae and acicula, and a trochophora-type larva, myzostomids are usually considered as annelids (e.g., Rouse and Fauchald, 1997). Recently, using 18S rDNA and elongation factor-1α DNA sequences, Eeckhaut et al. (2000) suggested that myzostomids are not annelids but a clade close to flatworms (a result supported later by Zrzavy et al., 2001, who placed myzostomids nested with Cycliophora, Rotifera, and Acanthocephala into the Platyzoa).

The taxonomy of Myzostomida (Jägersten, 1940) is largely based on the nature of their symbiotic associations. Jägersten (1940) considered myzostomids as a class of Annelida and distinguished two orders: the Proboscidea and the Pharyngidea (Table 1). Proboscidea consists of the single family Myzostomatidae, including more than 90% of the described species, most of them ectocommensals of crinoids. The Pharyngidea includes seven families, of which four are associated with crinoids: the Pulvinomyzostomatidae (represented by a single described species, parasitic in the digestive system), the Endomyzostomatidae (about 10 species infesting the integument), the Mesomyzostomatidae (two described species infesting gonads), and the Stelechopidae (one rare species, presumed to be ectocommensal). The remaining three Pharyngidea families are the Protomyzostomatidae (including five species, parasites of ophiuroid gonads), the Asteromyzostomatidae (five species, fixed at the surface of asteroids), and the Asteriomyzostomatidae (two species associated with asteroids, one parasitic of the digestive system, the other infesting the coelom).

A first phylogeny of Myzostomida was published by Jägersten (1940) and recently revisited by Grygier (2000) (Fig. 2). The latter research suggested that Pharyngidea contains three to four major clades and is paraphyletic with respect to Proboscidea (Fig. 2). None of these hypotheses are based on a statistical or cladistic analysis of characters, and all are based on morphology alone, which might expected to be homoplastic in a group with so many parasitic lineages. Using nuclear (18S rDNA) and mitochondrial (16S and COI) DNA sequence data from 37 myzostomid species representing 9 (out of 12) extant genera, we report here the first molecular phylogeny of this enigmatic group. The diversification of symbiotic echinoderm-myzostomid associations was then investigated by both parsimony- and likelihood-based character reconstruction methods.

MATERIALS AND METHODS

Taxon Sampling

Most of the specimens used in these analyses were hand-collected, with their hosts, by SCUBA diving at Morgat (Atlantic Ocean, France), Banyuls-sur-Mer (Mediterranean Sea, France), Hansa Bay (Bismarck Sea, Papua New Guinea), Toliara (Mozambique Channel, Madagascar), Lizard Island (Coral Sea, Australia), and around Japan (Table 2). Crinoids were examined under a binocular microscope, and the myzostomids were isolated, then preserved in 100% ethanol at 4°C. A few other specimens were provided by museums and preserved either in 70% ethanol or formaldehyde. In total, we analyzed 41 specimens belonging to 37 species (29 previously described and 8 new species) from 9 out of 12 extant genera (six families out of the eight existing). Genera not included here are *Asteriomyzostomum*

FIGURE 1. Light microscopy (LM) photographs of myzostomids on their host illustrating a few relevant lifestyles (A–F), and SEM views of various myzostomids (G–J) and of some of their organs (K–M). (A) *Myzostoma coriaceum*, an ectocommensal that moves on the external surface of crinoids with a preference to stay on the calyx close to cirri; these ectocommensal myzostomids divert food particles from the host's ambulacral grooves. (B, C) *M. furcatum* and *Myzostoma* sp., two ectocommensals that stand mostly on arms (B) or on pinnules (C). (D) A gall of *Endomyzostoma deformator* induced on *Metacrinus rotundus* at the level of an arm and at the base of a pinnule. (E) *Notopharyngoides aruensis* located in the anterior part of the digestive system of *Stephanometra oxyacantha*. (F) A body part of *Mesomyzostoma* sp. extending from a dissected gonadal pinnule of *Comanthus schlegelii*. (G) *Hypomyzostoma crosslandi* (ventral view), an ectocommensal living on crinoid pinnules. (H) *Mesomyzostoma* sp. (ventral view), an endoparasite living in crinoid celomic cavities. (I) *Myzostoma furcatum* (ventral view), an ectocommensal living on crinoid arms. (J) *Contramyzostoma sphaera* (dorsal view), an endoparasite living in the crinoid integument, where it induces the formation of a soft cyst. (K–M) *Myzostoma cirriferum* (an ectocommensal species): detailed view of the introvert (K), the margin of the trunk (L), and a parapodium (M). Scale bars: (A, B, C, E, F) 1 mm; (D) 1 cm; (G–J) 500 μm, (K–M) 100 μm. Abbreviations: a = crinoid arm; ag = anogenital pore; ant = anterior part; bp = buccal papillae; c = crinoid calyx; ci = marginal cirrus; cp = caudal process; ds = dorsal side; g = gall; i = introvert; lo = lateral organ; m = crinoid mouth; p = crinoid pinnule; pa = parapodium; pc = parapodial cone; pch = parapodial chaeta; pf = parapodial fold; post = posterior part; vs = ventral side.

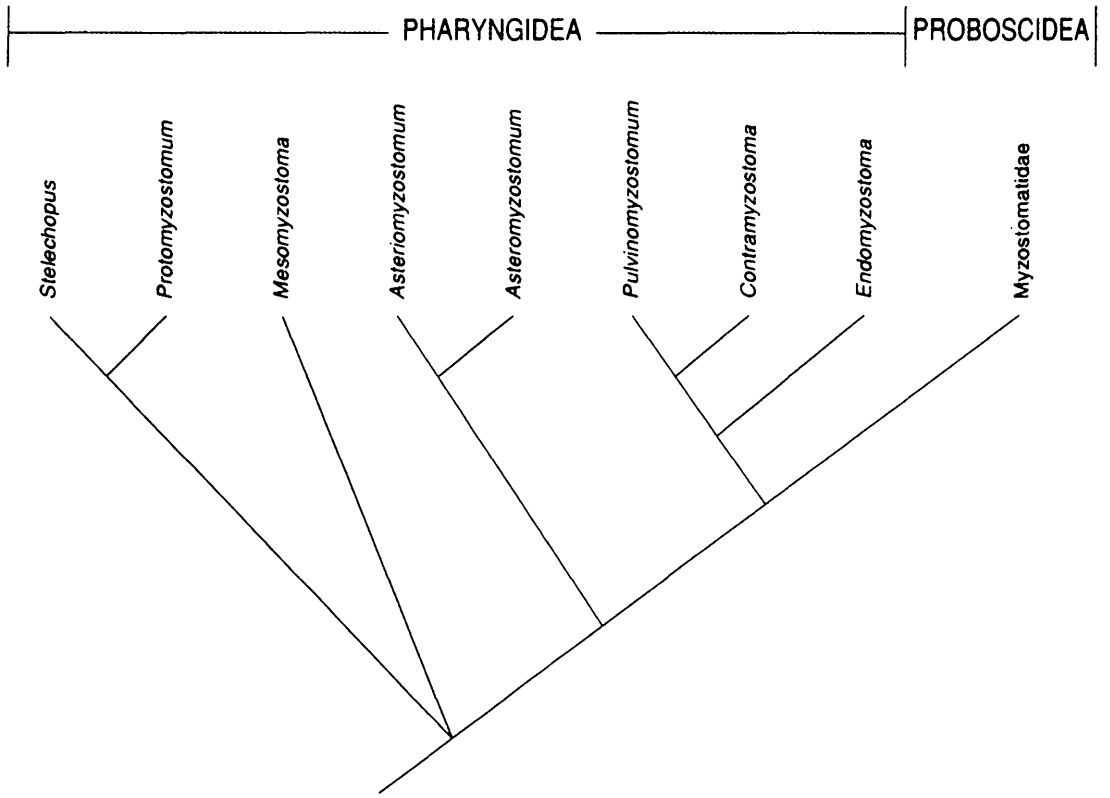

FIGURE 2. Phylogenetic relationships among the Myzostomida genera (following Grygier, 2000), based in part upon characters discussed by Jägersten (1940).

and *Stelechopus*, which include a total of three poorly known species, and *Mycomyzostoma*, which includes a single deep-sea species (Eeckhaut, 1998). Four species are each represented by two individuals differing in morphology or host species. The generic placement of the eight new species was determined on the base of morphological and ecological characters observed on living and fixed materials. Vouchers of the new species (and some others) are deposited at the South Australian Museum (SAM) and at the Belgian Royal Institute for Natural Sciences (IRSNB) (Table 2).

DNA Extraction, Polymerase Chain Reaction (PCR), and DNA Sequencing

Genomic DNA was extracted with organic solvents (Sambrook et al., 1989) or the DNeasy Tissue kit (QIAGEN). DNA fragments from the nuclear small ribosomal subunit (18S rDNA, ca. 1700 nucleotides), the mitochondrial large ribosomal subunit (16S rDNA, ca. 410 nucleotides), and the mitochondrial cytochrome oxidase I (COI, ca. 633 nucleotides) were amplified by PCR using Ready-To-Go PCR Beads (Pharmacia). Each PCR was performed in a volume of 25 μL containing 1.5 units of *Taq* DNA polymerase, 1 x PCR buffer (10 mM Tris/HCl, pH 9.0), 50 mM KCl, 1.5 mM $MgCl_2$, 0.20 mM of each dNTP, 0.6 pmol/μL of each primer, and 1 μL (~10 to 500 ng) of genomic DNA. PCR profiles were as follows: 5 min at 95°C followed by 35 to 40 cycles of 30 s at 95°C, 30 s at 40°C (COI), 50°C (16S), or 55°C (18S), and 60 to 90 s at 72°C. The 18S rDNA was amplified in three overlapping fragments of about 600 nucleotides each using primers from Eeckhaut et al. (2000). The universal primers 16Sar and 16Sbr (Palumbi et al., 1997) were used to amplify the 16S rDNA, and the primers LCO1490 and HCO2198 (Folmer et al., 1994) to amplify the COI. Amplification products were purified either with the Qiaquick PCR kit (QIAGEN) or from 1% agarose gels (Quantum Prep Freeze 'N Squeeze, Biorad). Both strands of each PCR product were directly sequenced using the BigDye Terminator Cycle Sequencing Kit (Applied Biosystems) and products were separated electrophoretically using an Applied Biosystems 3700 automated sequencer.

Sequences of the target 18S rDNA gene fragment were successfully obtained for 33 individuals, whereas smaller (<500 bp) fragments (not included in all analyses) were obtained for three additional specimens (Genbank DQ238147 to DQ238149). The sequence of *Myzostoma glabrum* was taken from Zrzavy et al. (1998) (Genbank AF116916). The sequence of *Myzostoma fissum*, *Myzostoma cirriferum*, *Contramyzostoma sphaera*, and *Notopharyngoides aruensis* were taken from Eeckhaut et al. (2000) (Genbank AF260584 to AF260587, respectively) (Table 3). Sequences of the target 16S rDNA and COI fragments were obtained for 30 and 33 specimens, respectively (Table 3). Sequences were edited with SEQPUP (Gilbert, 1996). All new sequences were deposited

TABLE 2. List of taxa examined in this study, along with their lifestyle, host, and collection locality.

Species	Lifestyle		Host	Collection locality
Mysostoma toliarense (Lanterbecq and Eeckhaut, 2003)	Endoparasitic living in soft cysts	(SCP)	*Comanthus parvicirra* (Müller, 1841) (CC)	Toliara (Mozambique Channel, Madagascar)
Myzostoma pseudocuniculus (Lanterbecq and Eeckhaut, 2003)	Ectocommensal on pinnules	(AE)	*Comanthus parvicirra* (Müller, 1841) (CC)	Toliara (Mozambique Channel, Madagascar)
Myzostoma cuniculus (Eeckhaut, Grygier, and Deheyn, 1998)	Ectocommensal on pinnules	(AE)	*Comanthus mirabilis* (Rowe, Hogget, Birtles, and Vail, 1986) (CC)	Lizard Island (Coral Sea, Australia)
Myzostoma nigromaculatum (Eeckhaut, Grygier, and Deheyn, 1998)	Ectocommensal on calyx	(GE)	*Phanogenia gracilis* (Hartlaub, 1890) (CC)	Hansa Bay (Bismarck Sea, Papua New Guinea)
Myzostoma ambiguum (Graff, 1887)	Ectocommensal on calyx	(GE)	*Oxycomanthus bennetti* (Müller, 1841) (CC)	Hansa Bay (Bismarck Sea, Papua New Guinea)
Myzostoma capitocutis (Eeckhaut, VandenSpiegel, and Grygier, 1994)	Ectocommensal on calyx	(GE)	*Phanogenia gracilis* (Hartlaub, 1890) (CC)	Hansa Bay (Bismarck Sea, Papua New Guinea)
Myzostoma fissum (Graff, 1884)	Ectocommensal on pinnules	(AE)	*Dichrometra flagellata* (Müller, 1841) (CC)	Hansa Bay (Bismarck Sea, Papua New Guinea)
Myzostoma mortenseni (Jägersten, 1940)	Ectocommensal on calyx	(GE)	*Clarkomanthus albinotus* (Rowe, Hogget, Birtles, and Vail, 1986) (CC)	Hansa Bay (Bismarck Sea, Papua New Guinea)
Myzostoma glabrum (Leuckart, 1842)	Ectoparasitic fixed on calyx	(FE)	*Antedon mediterranea* (Lamarck, 1816) (CC)	Banyuls-sur-Mer (Mediterranean Sea, France)
Myzostoma alatum (Graff, 1884)	Ectoparasitic fixed on calyx	(FE)	*Leptometra phalangium* (Müller, 1841) (CC)	Banyuls-sur-Mer (Mediterranean Sea, France)
Myzostoma cirriferum (Leuckart, 1827)	Ectocommensal on calyx	(GE)	*Antedon bifida* (Pennant, 1777) (CC)	Morgat (Atlantic Ocean, France)
Myzostoma polycyclus (Atkins, 1927)	Ectocommensal on calyx	(GE)	*Comanthus parvicirra* (Müller, 1841) (CC)	Hansa Bay (Bismarck Sea, Papua New Guinea)
Myzostoma laingense (Eeckhaut, Grygier, and Deheyn, 1998)	Ectocommensal on pinnules	(AE)	*Stephanometra oxyacantha* (Hartlaub, 1890) (CC)	Hansa Bay (Bismarck Sea, Papua New Guinea)
Myzostoma furcatum (Graff, 1887)	Ectocommensal on pinnules	(AE)	*Himerometra robustipinna* (Carpenter, 1881) (CC)	Lizard Island (Coral Sea, Australia)
Myzostoma coriaceum (Graff, 1884)	Ectocommensal on calyx	(GE)	*Comanthus schlegelii* (Carpenter, 1881) (CC)	Lizard Island (Coral Sea, Australia)
Notopharyngoides aruensis (Remscheid, 1918)	Endoparasitic living in digestive tube	(ADSE)	*Stephanometra oxyacantha* (Hartlaub, 1890) (CC)	Hansa Bay (Bismarck Sea, Papua New Guinea)
Hypomyzostoma fasciatum (Remscheid, 1918)	Ectocommensal on arms	(AE)	*Himerometra robustipinna* (Carpenter, 1881) (CC)	Lizard Island (Coral Sea, Australia)
Hypomyzostoma sp .aff. *crosslandi* a (Boulenger, 1913)	Ectocommensal on arms	(AE)	*Liparometra articulata* (Müller, 1849) (CC)	Lizard Island (Coral Sea, Australia)
Hypomyzostoma sp .aff.*crosslandi* b (Boulenger, 1913)	Ectocommensal on arms	(AE)	*Stephanometra spinnipinna* (Hartlaub, 1890) (CC)	Lizard Island (Coral Sea, Australia)
Hypomyzostoma n. sp.1 (SAM)	Ectocommensal on arms	(AE)	*Colobometra perspinosa* (Carpenter, 1881) (CC)	Lizard Island (Coral Sea, Australia)
Pulvinomyzostomum pulvinar (Graff, 1884)	Endoparasitic living in digestive tube	(ADSE)	*Leptometra phalangium* (Müller, 1841) (CC)	Banyuls-sur-Mer (Mediterranean Sea, France)
Contramyzostoma sphaera (Eeckhaut, Grygier, and Deheyn, 1998)	Endoparasitic living in soft cysts	(SCP)	*Comatella stelligera* (Carpenter, 1880) (CC)	Hansa Bay (Bismarck Sea, Papua New Guinea)
Endomyzostoma clarki (McClendon, 1906)	Endoparasitic living in galls	(GP)	*Metacrinus rotundus* (Carpenter, 1884) (SC)	Okinawa (Japan Sea, Japan)
Endomyzostoma tenuispinum (Graff, 1884)	Endoparasitic living in galls	(GP)	*Saracrinus nobilis* (Carpenter, 1882) (SC)	New Caledonia
Endomyzostoma deformator (Graff, 1884)	Endoparasitic living in galls	(GP)	*Endoxocrinus alternicirrus* (Carpenter, 1884) (SC)	Okinawa (Japan Sea, Japan)
Endomyzostoma n sp. 1 (IRSNB)	Endoparasitic living in soft cysts	(SCP)	Comasteridae (CC)	Toliara (Mozambique Channel, Madagascar)
Endomyzostoma cysticolum (Graff, 1883)	Endoparasitic living in cysts	(CCP)	*Promachocrinus kerguelensis* (Carpenter, 1888) (CC)	Antarctic Sea
Endomyzostoma n. sp. 2 (SAM)	Endoparasitic living in galls	(GP)	*Metacrinus rotundus* (Carpenter, 1884) (SC)	Okinawa (Japan Sea, Japan)
Endomyzostoma n. sp. 3 (SAM)	Ectocommensal on calyx	(GE)	*Metacrinus rotundus* (Carpenter, 1884) (SC)	Okinawa (Japan Sea, Japan)
Mesomyzostoma n. sp. 2 (SAM)	Endoparasitic living in gonads/celom	(ECC)	*Oxycomanthus* sp. (CC)	Okinawa (Japan Sea, Japan)
Mesomyzostoma katoi (Okada, 1933)	Endoparasitic living in gonads/celom	(ECC)	*Oxycomanthus japonica* (Müller, 1841) (CC)	Okinawa (Japan Sea, Japan)
Mesomyzostoma n. sp. 4b (SAM)	Endoparasitic living in gonads/celom	(ECC)	*Liparometra articulata* (Müller, 1849) (CC)	Lizard Island (Coral Sea, Australia)

(Continued on next page)

TABLE 2. List of taxa examined in this study, along with their lifestyle, host, and collection locality. (Continued)

Species	Lifestyle		Host	Collection locality
Mesomyzostoma n. sp. 3a (SAM)	Endoparasitic living in gonads/celom	(ECC)	*Comanthus schlegelii* (Carpenter, 1881) (CC)	Lizard Island (Coral Sea, Australia)
Mesomyzostoma n. sp. 3b (SAM)	Endoparasitic living in gonads/celom	(ECC)	*Comanthus schlegelii* (Carpenter, 1881) (CC)	Lizard Island (Coral Sea, Australia)
Mesomyzostoma reichenspergi (Remscheid, 1918)	Endoparasitic living in gonads/celom	(ECC)	*Himerometra magnipinna* (Clark, 1908) (CC)	Lizard Island (Coral Sea, Australia)
Mesomyzostoma n. sp. 4a (SAM)	Endoparasitic living in gonads/celom	(ECC)	*Dichrometra flagellata* (Müller, 1841) (CC)	Lizard Island (Coral Sea, Australia)
Mesomyzostoma n. sp. 1a (SAM)	Endoparasitic living in gonads/celom	(ECC)	*Clarkomanthus littoralis* (Carpenter, 1888) (CC)	Lizard Island (Coral Sea, Australia)
Mesomyzostoma n. sp. 1b (SAM)	Endoparasitic living in gonads/celom	(ECC)	*Clarkomanthus littoralis* (Carpenter, 1888) (CC)	Lizard Island (Coral Sea, Australia)
Protomyzostomum polynephris (Fedotov, 1912)	Endoparasitic living in gonads/celom	(ECC)	*Gorgonocephalus eucnemis* (Muller and Troschel, 1842) (O)	Murmansk (Barents Sea, Russia)
Protomyzostomum glanduliferum (Bartsch, 1995)	Endoparasitic living in gonads/celom	(ECC)	*Ophiacantha disjuncta* (Koehler, 1911) (O)	Weddel Sea (Antarctic)
Asteromyzostomum sp.	Ectoparasitic living in ambulacral grooves	(FE)	*Labidiaster* sp. (A)	Weddel Sea (Antarctic)

Vouchers of the new species (and some others) are deposited at the South Australian Museum (SAM) and at the Belgian Royal Institute for Natural Sciences (IRSNB). Lifestyle abbreviations: GE = General Ectocommensal (moving on the external surface of crinoids with a preference for staying on the crinoid calyx; these myzostomids divert food particles from the host's ambulacral grooves); AE. = Arm Ectocommensal (staying preferably on the pinnules, or the arms); FE = Fixed Ectoparasite (these myzostomids are externally fixed by their chaetae on the calyx of the crinoid, close to the host's mouth, from which they steal food particles, or attached in an ambulacral groove of a sea star); ADSE = Anterior Digestive System Endoparasite; ECC = Endoparasite of Celomic Cavities (generally in proximity or inside the host's gonads); SCP = Soft Cysticolous Parasites (living in a soft and uncalcified cyst located on crinoid's arms); CCP = Calcified Cysticolous Parasites (inducing a calcified cyst at the base of the crinoid's arms; this cyst is made of newly synthetized ossicles); GP = Gallicolous parasites (inducing a gall on arms by deformation of the original crinoid's ossicles). Host abbreviations: CC = Comatulid crinoid, SC = Stalked crinoid, O = Ophiuroid, A = Asteroid.

in Genbank under accession numbers DQ238114 to DQ238212 (Table 3).

DNA Sequence Alignments

Two types of alignments were considered, one to determine placement of the root with outgroup taxa, and a second, including only ingroup taxa, for establishing the relationships among myzostomids.

Annelids, platyhelminthes, acanthocephalans, and rotifers were selected as outgroup taxa based on existing hypotheses of their affinities with myzostomids (Rouse and Fauchald, 1997; Eeckhaut et al., 2000; Zrzavy et al., 2001). The outgroup sample was designed to place the root of the Myzostomida and not to understand the placement of this group in the larger metazoan tree (e.g., no bilaterians, ecdysozoans, or deuterostomes were sampled). The single 18S rDNA alignment considered for determining the placement of the myzostomid root was obtained as follows: (i) an alignment of 11 outgroup taxa and five myzostomids was obtained from the Antwerp SSUrRNA database (Van De Peer et al., 1998) that takes 18S rDNA secondary structure into account, and (ii) this alignment was used as a profile in ClustalX (Thompson et al., 1997), against which the new 33 myzostomid 18S rDNA sequences were aligned using default parameter settings. 16S rDNA and COI alignments were not considered here as both transversions (Tv) and transitions (Ti) sites in each gene appeared saturated (not shown).

The phylogenetic relationships among myzostomids were assessed using alignments including exclusively myzostomid taxa. COI sequences were aligned according to the corresponding amino acid alignment. 18S rDNA and 16S rDNA sequences were aligned with the program ProAlign (Löytynoja and Milinkovitch, 2003). This software implements a method for multiple sequence alignment that combines an HMM (hidden Markov model) approach, a progressive alignment algorithm, and a probabilistic evolution model describing the character substitution process. ProAlign allows for the computation of each column minimum posterior probability and columns with a posterior probability below a user-defined threshold can be excluded before phylogeny inference. We investigated the influence (on phylogeny inference) of excluding positions with minimum posterior probabilities (PP) < 0, 50, 70, and 90% (higher values reflecting more stringent exclusion criteria). We also used ProAlign for estimating the multiple alignment among the 49 sequences (11 outgroup taxa and 38 myzostomids, see above) of 18S rDNA to infer the reliability of the rooting obtained with the secondary structure-based alignment (see above). The characters excluded in the different datasets are summarized in Table 4. All alignments are available at the *Systematic Biology* website (http://systematicbiology.org/) or on request to the authors.

Phylogenetic Analyses

18S rDNA, 16S rDNA, and COI sequences were analyzed separately and in combination (Table 4). The incongruence length difference (ILD) test (Farris et al., 1994) was used to test for incongruence between the three genes. The test was implemented in PAUP*4.0b4a (Swofford, 1998) (partition homogeneity method with 100 replicates) and invariable characters were removed before starting the analysis (Cunningham, 1997).

TABLE 3. GenBank accession numbers of the Metazoa used in the analyses.

		Species	18S rDNA	16S rDNA	COI
Outgroup					
Annelida	Polychaeta	*Sabella pavonina*	U67144	—	—
		Glycera americana	U19519		
	Ochetostoma erythrogrammon (Echiura)		X79875	—	—
	Siboglinum fiordicum (Pogonophora)		X79876	—	—
	Clitellata	*Lumbriculus variegatus* (Oligochaeta)	AY040693	—	—
Plathelminthes	Turbellaria	*Dugesia japonica*	AF013153	—	—
	Trematoda	*Fasciola hepatica*	AJ004969	—	—
Rotifera	Monogononta	*Brachionus platus*	AF154568	—	—
	Bdelloidea	*Philodina acuticornis*	U41281	—	—
Acanthocephala	Archiacanthocephala	*Moniliformis moniliformis*	Z19562	—	—
		Oligacanthorhynchus tortuosa	AF064817	—	—
Ingroup					
Order	Family				
		Mysostoma toliarense	DQ238136	DQ238172	DQ238201
		Myzostoma pseudocuniculus	DQ238139	DQ238175	DQ238204
		Myzostoma cuniculus	DQ238138	DQ238174	DQ238203
		Myzostoma nigromaculatum	DQ238140	—	—
		Myzostoma ambiguum	DQ238142	—	DQ238206
		Myzostoma capitocutis	DQ238144	DQ238177	DQ238209
		Myzostoma fissum	AF260584	DQ238176	DQ238208
		Myzostoma mortenseni	DQ238143	—	DQ238207
		Myzostoma glabrum	AF116916	—	—
Proboscidea	Myzostomatidae	*Myzostoma alatum*	DQ238135	DQ238171	DQ238200
		Myzostoma cirriferum	AF260585	DQ238170	DQ238199
		Myzostoma polycyclus	DQ238137	DQ238173	DQ238202
		Myzostoma laingense	DQ238141	—	DQ238205
		Myzostoma furcatum	DQ238145	DQ238178	DQ238211
		Myzostoma coriaceum	DQ238146	DQ238179	DQ238212
		Notopharyngoides aruensis	AF260587	—	DQ238210
		Hypomyzostoma fasciatum	DQ238131	DQ238166	DQ238195
		Hypomyzostoma sp .aff. *crosslandi* a	DQ238133	DQ238168	DQ238197
		Hypomyzostoma sp .aff.*crosslandi* b	DQ238134	DQ238169	DQ238198
		Hypomyzostoma n. sp.1	DQ238132	DQ238167	DQ238196
	Pulvinomyzostomatidae	*Pulvinomyzostomum pulvinar*	DQ238114	DQ238150	DQ238180
		Contramyzostoma sphaera	AF260586	—	DQ238187
		Endomyzostoma clarki	DQ238124	DQ238159	DQ238188
		Endomyzostoma tenuispinum	DQ238128	DQ238163	DQ238192
	Endomyzostomatidae	*Endomyzostoma deformator*	DQ238126	DQ238161	DQ238190
		Endomyzostoma n sp. 1	DQ238129	DQ238164	DQ238193
		Endomyzostoma cysticolum	DQ238130	DQ238165	DQ238194
		Endomyzostoma n. sp. 2	DQ238125	DQ238160	DQ238189
Pharyngidea		Endomyzostoma n. sp. 3	DQ238127	DQ238162	DQ238191
		Mesomyzostoma n. sp. 2	DQ238120	DQ238156	DQ238186
		Mesomyzostoma katoi	DQ238121	—	—
		Mesomyzostoma n. sp. 3a	DQ238117	DQ238153	DQ238183
	Mesomyzostomatidae	*Mesomyzostoma* n. sp. 3b	DQ238115	DQ238151	DQ238181
		Mesomyzostoma reichenspergi	DQ238116	DQ238152	DQ238182
		Mesomyzostoma n. sp. 4a	DQ238118	DQ238154	DQ238184
		Mesomyzostoma n. sp. 4b	DQ238119	DQ238155	DQ238185
		Mesomyzostoma n. sp. 1a	DQ238122	DQ238157	—
		Mesomyzostoma n. sp. 1b	DQ238123	DQ238158	—
	Protomyzostomatidae	*Protomyzostomum polynephris*	DQ238149	—	—
		Protomyzostomum glanduliferum	DQ238148	—	—
	Asteromyzostomatidae	*Asteriomyzostomum* sp.	DQ238147	—	—

All our new sequences were deposited in GenBank under accession numbers DQ238114 to DQ238212.

MP analyses were performed with PAUP*4.0b4a (Swofford, 1998) using a heuristic search (SeqAdd and TBR branch-swapping). We also assessed the stability of the phylogenetic tree using the Goloboff (1993) fit criterion with heuristic searches and k = 0, 2, 4, 6, and 8. Clade supports were estimated by bootstrapping (Felsenstein, 1985) (Simple SeqAdd and TBR branch-swapping; 1000 replicates) and Bremer support (BS; Bremer, 1994).

Heuristic likelihood analyses (SeqAdd and branch-swapping) were performed using PAUP*4.0b4a (Swofford, 1998) with the likelihood model selected by ModelTest v3.6 (Posada and Crandall, 1998) and MrModelTest 1.0b (Nylander, 2002) (Table 4). The GTR model, with rate heterogeneity and estimated proportion of invariable sites (GTR+I+G model), was most often identified as best fitting the observed data (Table 4). Bootstrap analyses could not be performed

TABLE 4. Characteristics of the alignments.

	Multiple alignment program used	Stringency	Number of sequences	Number of sites excluded	Final aligned length (bp)	MP statistics: Number and percentage of variable sites	MP statistics: Number and percentage of parsimony-informative sites	Model of evolution selected by MrModeltest
Outgroup+Myzostomids								
18S rDNA	Secondary structure		49	0	2211	1063 (48%)	751 (34%)	/
	ProAlign	PP 0%	49	0	2091	1024 (49%)	719 (34%)	GTR+I+G
		PP 50%	49	791	1300	574 (44%)	380 (29%)	GTR+I+G
		PP 70%	49	921	1170	481 (41%)	315 (27%)	GTR+I+G
		PP 90%	49	1052	1039	389 (37%)	248 (24%)	GTR+I+G
18S rDNA	ProAlign	PP 0%	38	0	1791	408 (23%)	267 (15%)	GTR+I+G
		PP 50%	38	135	1656	321 (19%)	215 (13%)	GTR+I+G
		PP 70%	38	204	1587	275 (17%)	187 (12%)	HKY+I+G
		PP 90%	38	278	1513	246 (16%)	168 (11%)	GTR+I+G
Myzostomids only								
16S rDNA	ProAlign	PP 0%	30	0	444	237 (54%)	198 (45%)	GTR+G
		PP 50%	30	127	317	130 (41%)	110 (35%)	GTR+G
		PP 70%	30	151	293	114 (39%)	94 (32%)	GTR+I+G
		PP 90%	30	173	271	102 (38%)	82 (30%)	GTR+I+G
COI	Codon-based alignment		33	0	633	323 (51%)	282 (45%)	Codon model
18S rDNA + 16S rDNA + COI	ProAlign	PP 0%	38	0	2853	968 (34%)	747 (26%)	GTR+I+G
		PP 50%	38	262	2606	774 (30%)	607 (23%)	GTR+I+G
		PP 70%	38	355	2513	712 (28%)	563 (22%)	GTR+I+G
		PP 90%	38	451	2417	671 (28%)	532 (22%)	GTR+I+G

PP = Posterior probability used in ProAlign to exclude characters (positions with a posterior probability below the user-defined threshold of 0, 50, 70, or 90% are excluded). Models abbreviations: GTR = General time-reversible model (Rodriguez et al., 1990). HKY = Hasegawa et al.'s (1985) model. I = proportion of invariable sites. G = gamma distribution of rates for variable sites. / = not tested with MrBayes.

with PAUP*4.0b4a because it would have required unpractical computing times.

ML analyses were also performed using the Metapopulation Genetic Algorithm (MetaGA; Lemmon and Milinkovitch, 2002) using the software Metapiga 1.0.2b (http://www.ulb.ac.be/sciences/ueg/html_files/softwares.html) with the following settings: four populations of four individuals each, probability consensus pruning, random starting trees, HKY nucleotide substitution model (i.e., the most parameter-rich model implemented in MetaGA), with estimated proportion of invariable sites and rate heterogeneity (four categories). MetaGA branch support values (PBS, which approximate posterior probabilities of branches) were computed from 1,000 MetaGA samples (250 replicates with four populations).

Bayesian analyses were performed with MrBayes v3.0b4 (Ronquist and Huelsenbeck, 2003). The model selected by MrModelTest 1.0b (Nylander, 2002) was applied for each specific dataset. Four Markov chains were run simultaneously for 5×10^5 generations, and trees were sampled every 100 cycles for a total of 5,000 trees. The first 1,000 trees with preasymptotic likelihood scores, i.e., the 100,000 first generations, were discarded as "burn-in." The remaining trees were used to compute Bayesian posterior probabilities (BPP) for each clade of the consensus tree. The run was repeated twice to ascertain convergence towards the same posterior parameter distribution (see Huelsenbeck et al., 2002).

Evolution of Symbiosis

Several optimization methods are available for reconstructing ancestral traits (see Cunningham et al., 1998; Crisp and Cook, 2005, for a review). We used MacClade 4.0 (Maddison and Maddison, 2000) and Mesquite 1.0 (Maddison and Maddison, 2004) to reconstruct the evolution of characters associated with symbiosis, both under maximum parsimony and maximum likelihood criteria. Parsimony reconstruction methods find, for each internal node, the ancestral state(s) that minimizes the number of character changes given the tree and observed character distribution, whereas likelihood methods find the ancestral state(s) that maximizes the probability of the observed states (at terminal nodes) evolving under a defined stochastic model of evolution (Pagel, 1999). Likelihood modeling of traits has several advantages over parsimony, e.g., indicating probabilities of alternative states (see Ronquist, 2004; Crisp and Cook, 2005). Unordered states were used for MP, whereas the Markov k-state 1-parameter model, corresponding to Lewis's (2001) Mk model, was used for the ML reconstruction. MP reconstruction was made on the MP tree of Figure 4A and ML reconstruction on the Bayesian phylogram of Figure 5. Both trees were obtained from analyses of the combined (18S + COI + 16S) dataset (PP threshold of 90%), and the position of *Protomyzostomum polynephris*, *P. glanduliferum*, and *Asteriomyzostomum* sp. was estimated from analyses on the 18S matrix only (see Fig. 6).

We defined eight possible character states of symbiotic lifestyles for adult specimens of myzostomids (see details in Fig. 1 and Table 2): general ectocommensal (GE), arm ectocommensal (AE), fixed ectoparasite (FE), anterior digestive system endoparasite (ADSE), endoparasite of celomic cavities (ECC), soft cysticolous parasites (SCP), celcified cysticolous parasites (CCP), and gallicolous parasites (GP). To investigate the evolution of host affiliation, we defined four possible host-preference character states: comatulid crinoid, stalked crinoid, ophiuroid, and asteroid.

We compared various ML-constrained trees to optimal ML trees using the Shimodaira-Hasegawa (SH) tests implemented in PAUP* (RELL model, 1000 replicates) (Shimodaira and Hasegawa, 1999). The first six constraints concern myzostomid lifestyles: (A) monophyly of the twenty parasitic myzostomids, (B) monophyly of the two endoparasites living in the digestive system, (C) monophyly of the nine endoparasites living in the gonads, (D) monophyly of the seventeen ectocommensals, (E) monophyly of the four endoparasites living in cysts, and (F) monophyly of the four endoparasites living in galls. We also tested the monophyly of the following multispecies genera: *Hypomyzostoma* (constraint G), *Myzostoma* (constraint H), *Mesomyzostoma* (constraint I), and *Endomyzostoma* (constraint J). Finally, we tested the reciprocal monophyly of the orders Pharyngidea and Proboscidea (constraint K). The "converse" command in PAUP* was used to test the nonmonophyly when the monophyly was already present in the optimal tree (constraints C', I', and J'). Cladistic topology-dependent permutation tail probability test (T-PTP) (Faith, 1991; Faith and Trueman, 1996) was performed as a complementary test to analyze and compare these alternative phylogenetic hypotheses.

RESULTS

Rooting of the Myzostomid Clade

Virtually all analyses (MP, MetaGA, and Bayesian analyses) of the 18S rDNA secondary-structure alignment support the rooting of the myzostomid subtree on a lineage including all the *Endomyzostoma* species plus *Pulvinomyzostomum pulvinar* (Fig. 3). The only exceptions appear in Bayesian analyses conducted with the most stringent ProAlign conditions (PP thresholds of 50, 70, and 90%). In these cases the root is located at the base of a clade including six of the seven *Endomyzostoma* species, whereas *Endomyzostoma* n. sp. 2 and *Pulvinomyzostomum pulvinar* are then positioned at the base of the clade grouping the remaining myzostomids species. Expected relationships between outgroup taxa found in recent phylogenetic analyses are recovered: Platyhelminthes are monophyletic and associated with Rotifera and Acanthocephala (Baguñà and Riutort, 2004), Rotifera are paraphyletic with regards to Acanthocephala (Garey et al., 1996; Garey et al., 1998), and Echiura and Pogonophora cluster with Annelida (McHugh, 1997) (Fig. 3).

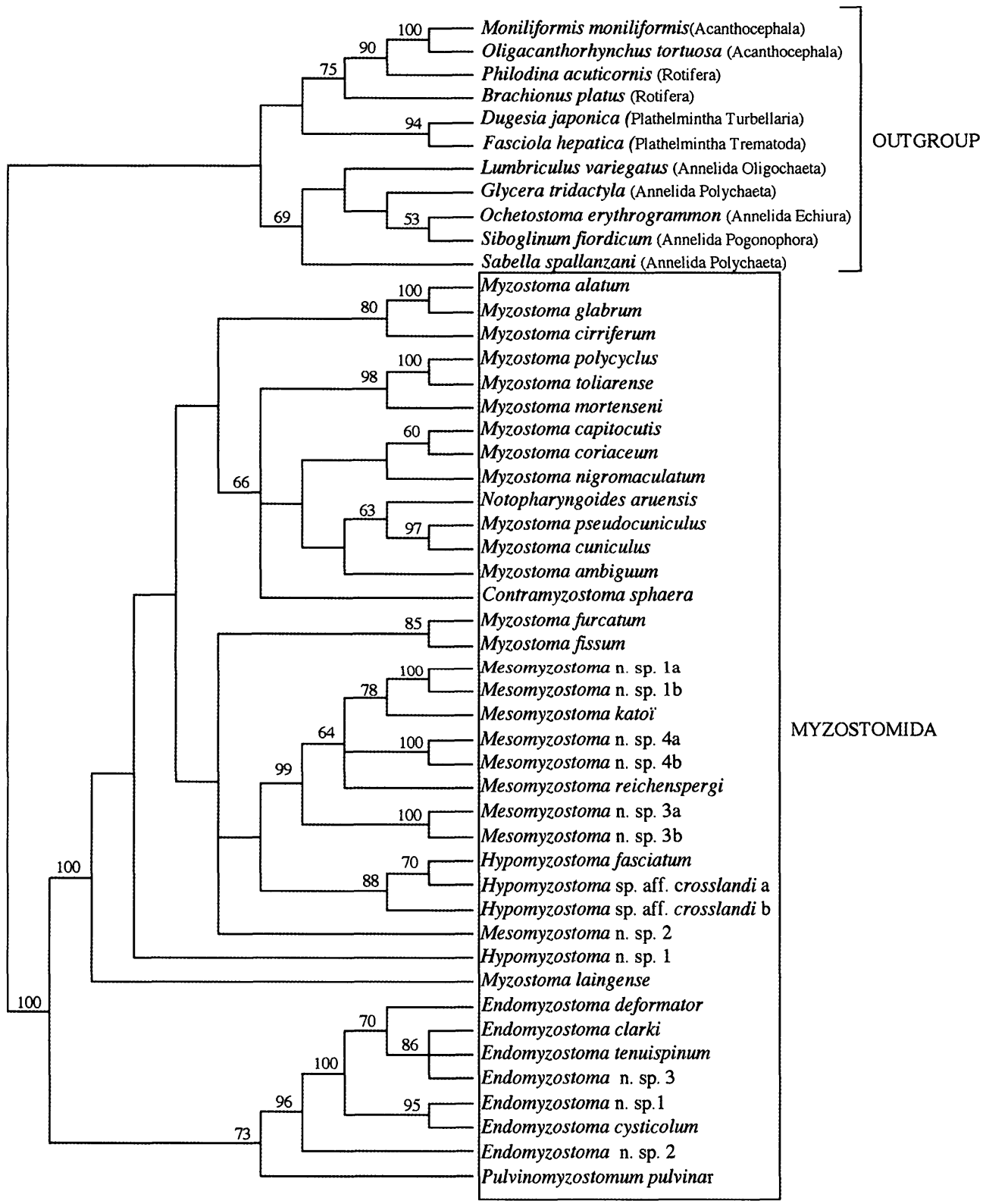

FIGURE 3. Rooting of the Myzostomida tree. Strict consensus among the six MP trees (38 ingroup taxa, 11 outgroup taxa) using the 18S rDNA alignment based on secondary structure (tree length = 2,957, CI = 0.5749, RI = 0.7602). Likelihood analyses (MetaGA and Bayesian) produced topologies similar to this one. Numbers above branches indicate bootstrap values >50% (1,000 replicates).

Phylogeny of the Myzostomida

Within Myzostomida, uncorrected pairwise sequence divergences are higher for 16S rDNA (0.25% to 28.4%), and COI (0.18% to 25%) than for 18S rDNA (0.058% to 14%). Saturation plots (data not shown) for each of the three genes, as well as the third positions of the COI codons, indicate no obvious Ti or Tv saturation for the whole range of pairwise distances. The ILD test showed that the three gene fragments were not significantly incongruent (ILD $P = 0.32$) and could consequently be combined in a three-gene dataset.

Combined analyses.—MP analyses with the most conservative alignments (i.e., excluding columns supported by posterior probabilities, PP < 90%, cf. Material and Methods) yielded five equally parsimonious trees (length = 2,287, 532 parsimony-informative sites, consistency index, CI = 0.41). The MP bootstrap 50% majority-rule consensus tree (1,000 replicates, each with 10 random-addition sequences) is shown in Figure 4A. Myzostomids are separated into two major clades: clade 1 (supported by a BV = 73% in the rooted tree, cf. Fig. 3) includes all *Endomyzostoma* species with *Pulvinomyzostomum* pulvinar as a sister group, whereas clade 2 (supported by a BV = 100% in the rooted tree, cf. Fig. 3) includes all other myzostomids. Note that this partition between the two major lineages of myzostomids is supported in the unrooted tree (Fig. 4a) by a BV = 100% and BS = 40. Most nodes within clade 1 are well supported by bootstrap values (>80%) and decay indices (Fig. 4a), except clade 13 (BV = 63). The two subclades within clade 2 are weakly supported (BV = 48% and 61% for clades 3 and 4, respectively). Clade 4 contains three European species that live at the surface of comatulid crinoids. Clade 3 mostly contains Indo–West Pacific species and further splits into clades 5 and 6 (not supported by BV). The former consists of seven species: five ectocommensals belonging to the genus *Myzostoma, Notopharyngoides aruensis* (a parasite of the crinoid digestive system), and *Contramyzostoma sphaera* (a cysticolous parasite of crinoid integument). Clade 6 contains one group of four ectocommensals (clade 7) of the *Myzostoma* genus and one group made of species belonging to three different genera (*Myzostoma, Mesomyzostoma*, and *Hypomyzostoma*) (clade 8). The genera *Mesomyzostoma* (crinoid gonad parasites) and *Hypomyzostoma* (ectocommensals) each form a monophyletic group (clades 24 and 33, respectively), although the latter is weakly supported by bootstrapping. *Myzostoma laingense*, a large species living preferentially on crinoid arms, branches off at the base of the *Mesomyzostoma* clade. The *Hypomyzostoma* group clusters with *M. fissum* and *M. furcatum*, two species with caudal processes that mimic crinoid pinnules. Variations in tree topologies under Goloboff weighting are due to the unstable positioning of *M. laingense* (often located at the base of clade 2) and of the three European myzostomids (clade 4) that often cluster with the Indo-Pacific myzostomids of clades 5 and 7.

The topology and support values of the MP tree illustrated in Figure 4a are very stable to inclusion of aligned columns with PP values <90% (see Table 5).

MetaGA maximum likelihood analyses are summarized in Figure 4b. All clades present in the MP tree are also present in the MetaGa tree. Clades supported in the MP analysis by bootstrap values >70% are also strongly supported by MetaGA branch support values (~90%). Differences between the MP and ML trees are (i) the absence of clade 5 in ML tree, and (ii) in clade 17 of the ML tree, *M. capitocutis* groups with *M. coriaceum*. The results of the MetaGA analyses are very stable to variation of the alignment stringency: excluding columns with a posterior probability <70, 50, or 0% (the latter representing the ProAlign alignment with no exclusion of characters) yielded topologies and branch support values (see Table 5) very similar to those obtained with the PP90% alignment (Fig. 4b). On the base of the MP and

TABLE 5. Clade support values under the MP, MetaGA, and Bayesian analyses of the four three-gene datasets.

	PP 90%			PP 70%			PP 50%			PP 00%		
	BV	PBS	BPP	BV	PBS	BPP	BV	PBS	BPP	BV	PBS	BPP
1	100	100	100	100	100	100	100	100	100	100	100	100
2	100	100	100	100	100	100	100	100	100	100	100	100
3	48	69	56	54	67	100	58	71	88	49	53	89
4	61	96	61	67	99	57	70	100	—	75	100	82
5	10	—	—	—	—	—	—	—	—	—	—	—
6	11	38	—	16	53	52	19	—	65	—	—	—
7	37	94	84	41	96	100	53	97	93	52	92	100
8	61	96	56	66	98	100	71	98	88	72	99	100
9	100	99	100	100	100	100	100	100	100	100	100	100
10	100	100	100	100	100	100	100	100	100	100	100	100
11	89	100	—	90	100	—	95	100	—	94	100	—
12	100	100	100	100	100	100	100	100	100	100	100	100
13	63	97	78	63	96	77	62	97	78	68	98	70
14	100	100	100	100	100	100	100	100	100	100	100	100
15	47	98	62	47	98	66	56	96	68	55	97	97
16	55	100	100	60	100	100	55	100	100	60	100	100
17	85	98	84	85	98	100	96	98	97	98	97	100
18	65	—	83	63	—	99	89	—	97	96	68	100
18*	—	84	—	—	83	—	—	59	—	—	—	—
19	88	100	100	86	99	100	90	100	100	99	99	100
20	86	99	—	85	99	—	96	98	70	91	97	—
21	100	100	100	100	100	100	100	100	100	100	100	100
22	27	69	—	32	73	—	28	55	—	—	32	—
23	19	47	—	29	74	56	29	69	—	22	48	—
24	80	100	100	76	100	100	78	99	100	79	100	100
25	100	100	100	99	100	100	100	99	100	100	100	100
26	100	100	100	100	100	100	100	100	100	100	100	100
27	23	39	—	24	—	—	—	—	47	—	36	34
28	31	67	—	27	70	31	37	78	—	—	—	—
29	99	100	100	100	100	100	100	100	100	100	100	100
30	61	80	67	60	76	61	75	91	90	73	84	96
31	100	100	100	100	100	100	100	100	100	100	100	100
32	77	100	100	78	99	100	77	100	100	98	100	100
33	16	66	—	22	78	48	—	—	—	—	—	—
34	50	98	100	51	99	100	49	100	100	80	100	100
35	100	100	100	99	100	100	100	100	100	100	100	100
36	100	100	100	100	100	100	100	99	100	100	100	100

PP = Posterior probability used by ProAlign (with thresholds of 0, 50, 70, and 90%). BV = Bootstrap value of MP analyses. PBS = Posterior branch support value of ML analyses with Metapiga. BPP = Bayesian posterior probability. — = Clade absent from the analysis. The numbers 1 to 36 refer to clades in Figures 4 and 5. *Difference of branching between the MP and MetaGA trees (Fig. 4).

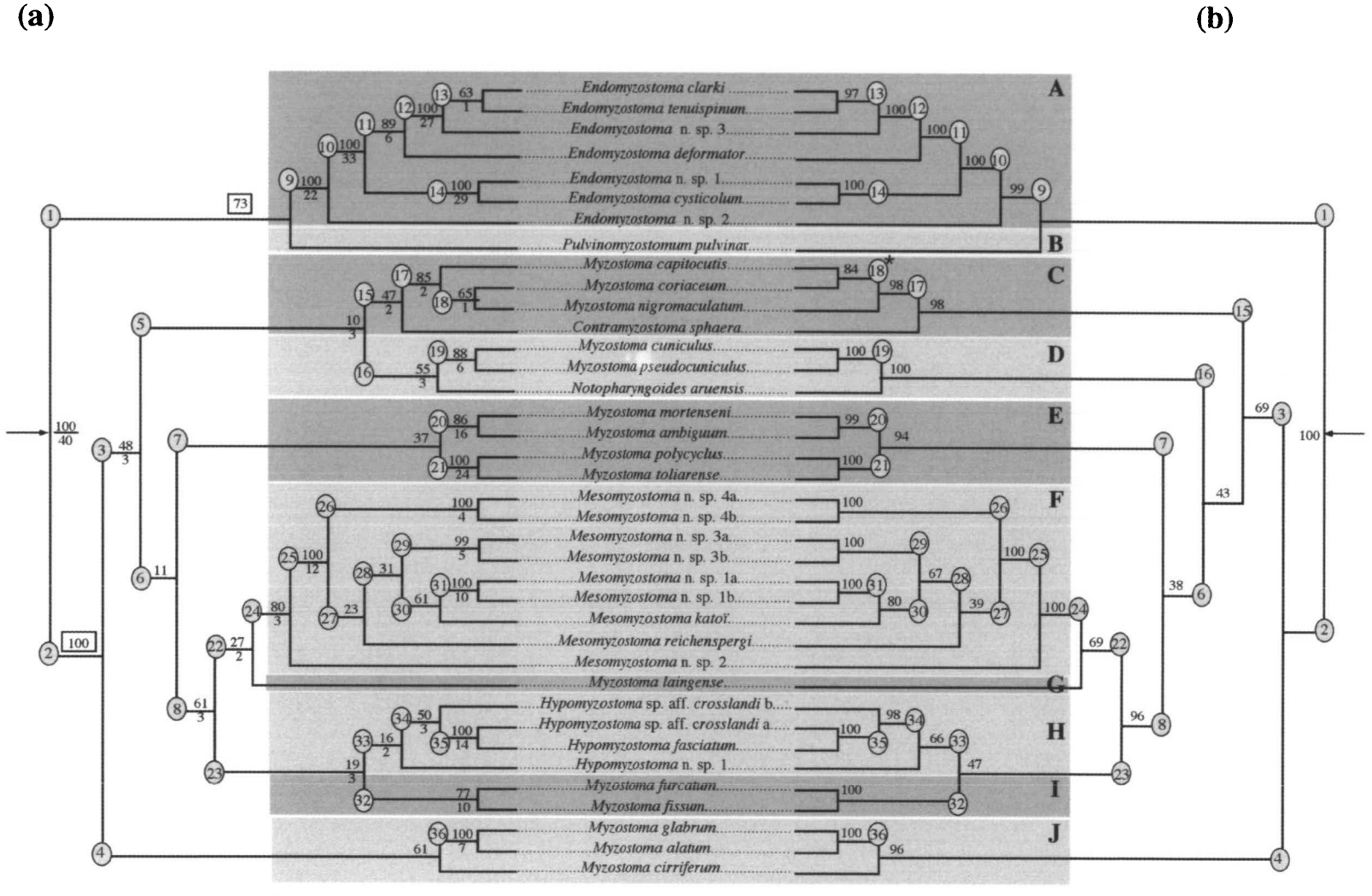

FIGURE 4. Phylogenetic analyses of the myzostomids three-gene dataset (PP threshold of 90%, see Table 4). (a) MP tree (bootstrap 50% majority-rule consensus tree, length = 2,287, CI = 0.41, RI = 0.63). Numbers above and below branches indicate bootstrap values (1,000 replicates) and Bremer support, respectively. (b) ML tree with MetaGA branch support values indicated above branches. Clades are numbered to facilitate comparison between the two trees. Squared BVs are those obtained from the rooted tree of Figure 3. Letterings A to J emphasize groups that are observed in most of the analyses. The asterisk indicates a difference of branching between the MetaGA and MP trees. Arrows indicate the root of the tree.

ML trees, we defined 10 major lineages of myzostomids (clades A to J; Fig. 4).

Bayesian likelihood analyses on the PP 90% aligment are summarized in Figure 5. The major lineages identified on the MP and MetaGA trees (clades A to J; Fig. 4) are also present in the consensus tree obtained with the Bayesian analyses (and supported by Bayesian Posterior Probabilities), except that *Hypomyzostoma* appears paraphyletic (H* in Fig. 5). Differences with the MP and MetaGA tree topologies concern position of *Endomyzostoma deformator*, of *Myzostoma ambiguum*, and of *Myzostoma laingense*.

Analyses of single-gene datasets.—In all analyses (MP, MetaGA, and Bayesian analyses) made on the single-gene datasets, the partition *Endomyzostoma* + *Pulvinomyzostomum* verses all other myzostomids is inferred,

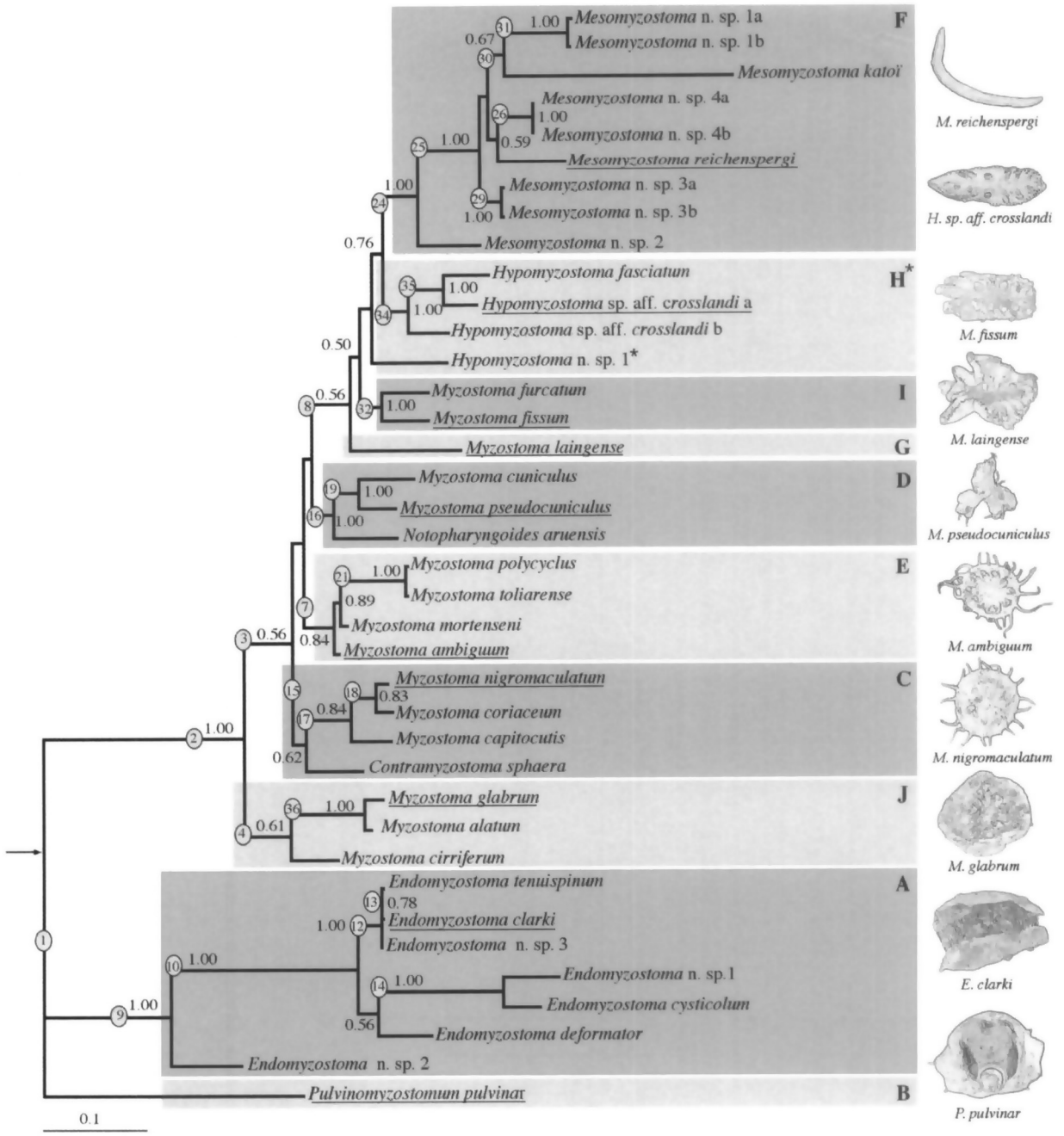

FIGURE 5. Bayesian likelihood analysis of the three-gene dataset (sites with minimum posterior probability <90% were excluded with ProAlign, see Table 4) using the specific model for each gene as selected by MrModelTest 1.0b (i.e., GTR+I+G for 18S and 16S, and the codon model for COI). Bayesian posterior probabilities (BPS) are indicated above nodes. Analyses of the other alignments (excluding sites with PP < 0, 50, and 70%) produced topologies identical to this one and similar BPS. A to J emphasize clades that are observed in most of the analyses. Outline of one species (name underlined) whose morphology is representative of the corresponding group is illustrated on the right of the tree. Arrow indicates the root of the tree. The branch lengths are proportional to the number of substitutions per site (see scale in figure).

whereas *Hypomyzostoma* (clade H) and *Mesomyzostoma* (clade F) are not always monophyletic. Among the eight groups, A and D are present in all single-gene analyses, whereas clade J is not supported by COI. The most obvious differences between the trees obtained with the combined dataset and those resulting from single-gene analyses concern weakly supported clades (e.g., clades 3, 5, 6, 8, 15; Fig. 4a). In general, the support of clades and resolution of trees is lower with the rapidly evolving mitochondrial single genes than with 18SrDNA.

Figure 6 illustrates the results of a Bayesian analysis made on an 18S rDNA dataset including the two ophiuroid parasites, *Protomyzostomum glanduliferum* and *P. polynephris*, and the asteroid ectoparasite,

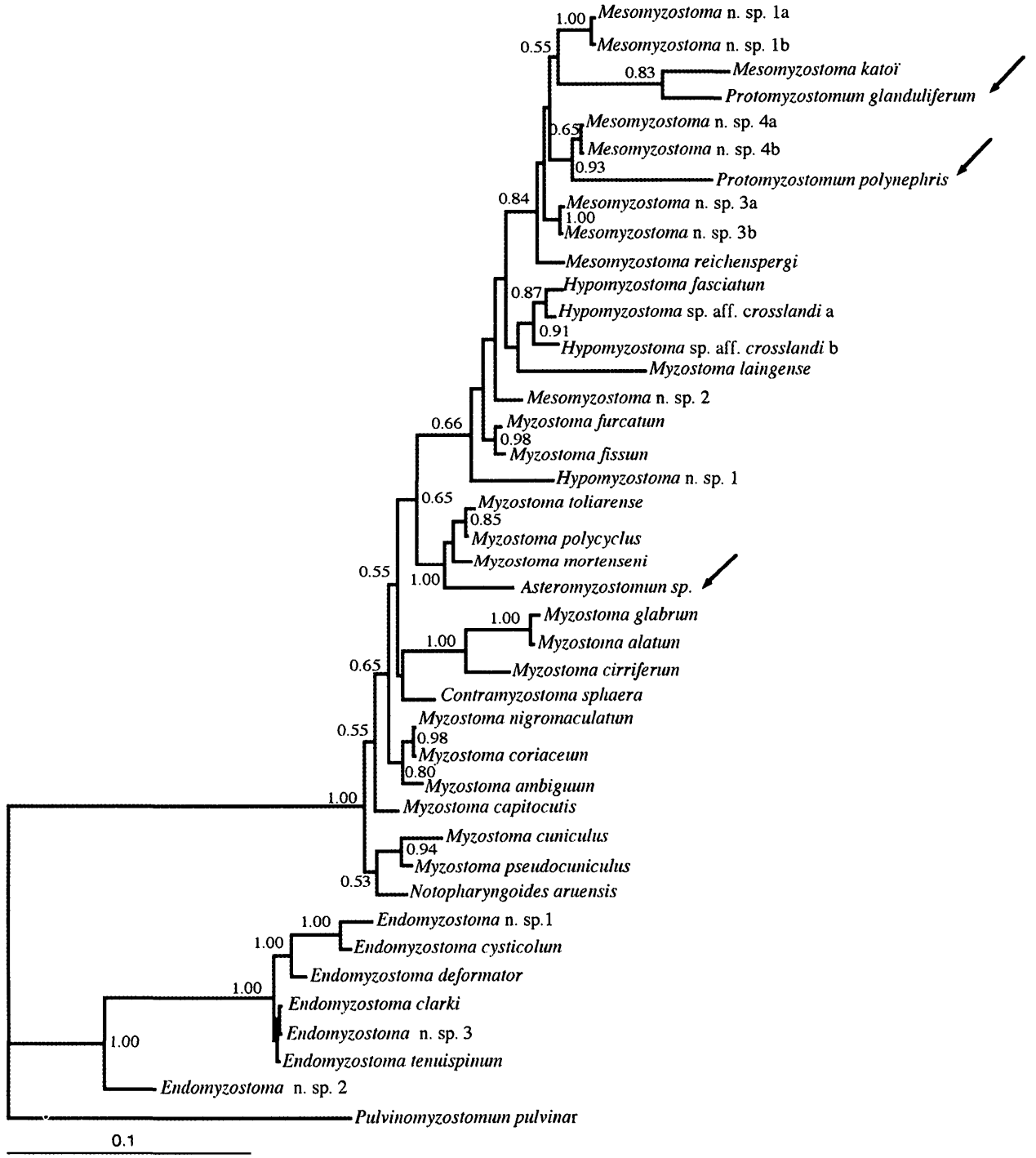

FIGURE 6. Bayesian likelihood analysis of the 18S rDNA dataset. Posterior probabilities are indicated above nodes. Arrows indicate the position of the two ophiuroid gonad parasites and the sea star parasite (for which 16S and COI are missing). The branch lengths are proportional to the number of substitutions per site (see scale in figure).

Asteromyzostomum sp. Note that as we had access only to formaline-preserved specimens of these three species, we could sequence only ca. 400 bp of the 18S gene (358 bp for the two *Protomyzostomum* species, of which 285 were constant and 49 parsimony-informative, and 497 bp for *Asteromyzostomum* sp., of which 377 were constant and 83 parsimony-informative), and failed to PCR amplify the 16S and COI fragments. The tree illustrated in Figure 6 suggests that the ophiuroid gonad parasites do not form a clade while the sea star ectoparasite, *Asteromyzostomum* sp., groups with crinoid ectocommensals. Similar results are obtained under MP and MetaGA analyses.

Evolution of Symbioses

Figure 7A illustrates the MP reconstruction of symbiotic lifestyles, mapped on the molecular phylogeny inferred from the combined dataset (18S, 16S, COI). The lifestyle reconstruction is equivocal for the ancestor of all extant myzostomids as well as in three other branches of the tree (two in *Endomyzostoma/Pulvinomyzostomum* clade; Fig. 7B and C, respectively, and one in the other clade). ML inference of the most likely ancestral state, however, suggests that a general ectocommensal lifestyle is the basal condition for myzostomids (relative likelihood = 0.38, whereas the state "gallicolous" is assigned a relative likelihood of 0.20). This myzostomid ancestor probably moved easily on the external surface of crinoids, as do some of the extant ectocommensals. Multiple specializations evolved from generalist ancestors. Hard cysticolous and some soft cysticolous parasites (*E. cysticolum* and *Endomyzostoma* n. sp. 1) probably evolved from a gallicolous (yellow in Fig. 7A) ancestor, whereas *Endomyzostoma* n. sp. 3 reverted to the general ectocommensal lifestyle. The body shape of the latter is similar to that of ectocommensal *Myzostoma* species (it is

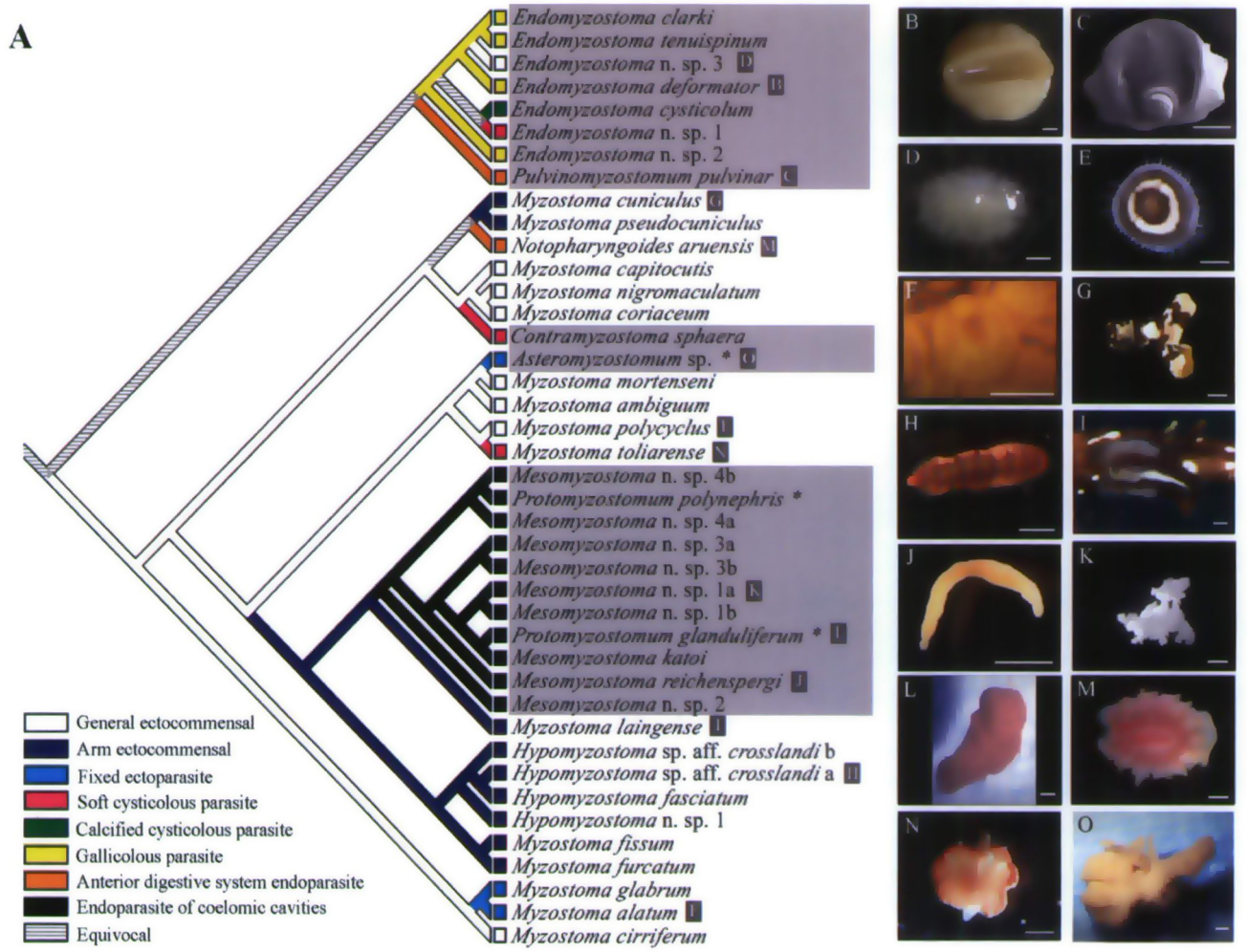

FIGURE 7. MP reconstruction of the evolution of myzostomid symbiotic lifestyles (A) and microscopic views of myzostomid species (B–O are LM views except C, which is a scanning electronic microscopy view). Grey boxes indicate members of the order Pharyngidea while all other species are members of the order Proboscidea. Asterisks indicate that the phylogenetic positions of *Protomyzostomum polynephris* and *P. glanduliferum* (parasites of ophiuroid gonads), and of *Asteriomyzostomum* sp. (infesting the ambulacral groove of sea stars) have been estimated only from 18S rDNA data (*cf.* Table 4 and Fig. 6). Letters in grey frames indicate species corresponding with pictures on the right. Scale bars: 1 mm.

flat, ovoid, exhibits parapodia, and is observed around the crinoid calyx; Fig. 7D). The evolution of symbiotic lifestyle within the remaining of myzostomids is almost totally resolved. The ancestor is a general ectocommensal worm that probably moved easily on the external surface of crinoids, as some of the extant ectocommensals do (white on Fig. 7A; Fig. 7E illustrates such type of ectocommensal). Specialized fixed ectoparasites (light blue in Fig. 7A) evolved twice independently; extant worms exhibiting this specialization stand around the crinoid mouth from where they divert food particles (Fig. 7F) or are associated with sea stars (*Asteromyzostomum* sp., Fig. 7O) on which they attach with processes of their lip. Specialized settlement on crinoid arms or pinnules (dark blue in Fig. 7A) also evolved twice independently: once in a clade represented by *M. cuniculus* and *M. pseudocuniculus*, two small species whose posterior body develops processes that resemble crinoid pinnules (Fig. 7G), and once in a diverse group of species that either develop alternating dark and white transversal bands that mimic crinoid arm ossicles (as in *Hypomyzostoma* species; Fig. 7H) or acquire caudal processes that resemble pinnules (e.g., *Myzostoma laingense;* Fig. 7I). Celom parasites (black in Fig. 7A) evolved from the arm/pinnule ectocommensals. *Mesomyzostoma* species most often infest the coelom in proximity to the gonads (note that crinoid gonads are located within the basal pinnules), and sometimes the gonads themselves (Fig. 7J). *Mesomyzostoma* n. sp. 1 (Fig. 7K) is particularly spectacular as it exhibits multiple lateral and caudal processes that deeply extend into the celomic ducts of the crinoid calyx such that only parts of the body can be separated from the host during dissections (G. Rouse, personal observation). Note that in this group of celomic parasites, a host shift from crinoids to ophiuroids (asterisks in Fig. 7A, illustrated in Fig. 7L) occurred twice independently. Finally, parasites of the crinoid digestive system (*N. aruensis* in Fig. 7M; *P. pulvinar* in Fig. 7C) as well as soft cysticolous parasites (e.g., *M. toliarense*, Fig. 7N) evolved multiple times independently.

Figure 8 illustrates the evolution of host preference in myzostomids. MP and ML inferences suggest that myzostomids first infested comatulid crinoids followed by either two independent host shifts towards stalked crinoids or a single host shift followed by a reversal towards comatulid infestation. Clearly, noncrinoid (asteroid, ophiuroid) parasitism appeared multiple times independently.

Additional material showing ML character reconstruction results is available at the *Systematic Biology* website (http://systematicbiology.org/).

Constrained Trees Analyses

Clearly, Shimodaira-Hasegawa (SH) tests confirm multiple independent emergence of parasitism in myzostomids. Best trees obtained under ML are statistically better than trees in which monophyly was imposed to any of the following groups: the 20 parasitic myzostomids, the 2 endoparasites living in the digestive system, the 19 ectocommensals, the 4 endoparasites living in cysts, and the 4 endoparasites living in galls. Similarly, the monophyly of the genus *Myzostoma* and of the two orders (Proboscidea and Pharyngidea) must be rejected. On the other hand, the nonmonophyly of *Mesomyzostoma*, and that of *Endomyzostoma* and *Hypomyzostoma* genera, cannot be rejected with statistical significance.

Furthermore, T-PTP tests suggest that all constrains can be rejected except for the nonmonophyly of *Mesomyzostoma* and of *Endomyzostoma.*

Discussion

Jägersten (1940) divided the Myzostomida into the orders Pharyngidea and Proboscidea on the base of differences in the anterior body ontogenesis of a few *Myzostoma* species (Proboscidea) and of *Pulvinomyzostomum pulvinar* (Pharyngidea). He observed that a proboscis differentiates in Proboscidea, whereas an extrusive pharynx develops in Pharyngidea: the blastopore (that becomes the mouth) is located at the apex of the introvert in *Myzostoma* species, whereas it forms the ventral opening through which the pharynx is extrude in *P. pulvinar*. Jägersten (1940) then built a classification in which all *Myzostoma* species are separated from all the other genera (for most of which the ontogeny of the anterior body part was however unknown). Since then, authors have described new myzostomid species, without a detailed knowledge of their ontogeny, and created new genera that were more or less haphazardly placed in one of the two orders. Generally, parasites are considered as Pharyngidea and ectocommensals as Proboscidea. We here demonstrate that neither Pharyngidea (hence, the emergence of parasitism) nor Proboscidea are monophyletic groupings. *Endomyzostoma* is a monophyletic taxon, whereas *Mesomyzostoma* is not, unless the ophiuroid-associated *Protomyzostomum* is renamed and placed in the genus *Mesomyzostoma*. The genus *Hypomyzostoma* could be monophyletic, although only one step is necessary to make it paraphyletic with respect to three *Myzostoma* species (*M. laingense, M. fissum*, and *M. furcatum).* As we investigated here only one species from each of *Contramyzostoma* and *Notopharyngoides* (including two and five described species, respectively), we could not test their monophyly. Specimens of two monotypic genera (*Mycomyzostoma calcidicola* and *Stelechopus hyocrini*; both infesting stalked crinoids) as well as the genus *Asteriomyzostomum* (including two species infesting the pyloric caeca of sea stars; Stummer-Traunfels, 1903; Wheeler, 1905) still need to be investigated. Our analyses demonstrate that the traditional classification of myzostomids, especially the division into two orders (Pharyngidea and Proboscidea), needs to be extensively revised. Waiting for an extensive analysis of the evolution of the myzostomid body plans for assisting the establishment of a classification, we suggest to limit the order Pharyngidea to the *Endomyzostoma* and *Pulvinomyzostomum* species (group AB in Fig. 4). Following our molecular phylogenetic analyses we also suggest (i) the erection of a new taxon grouping *Mesomyzostoma* and

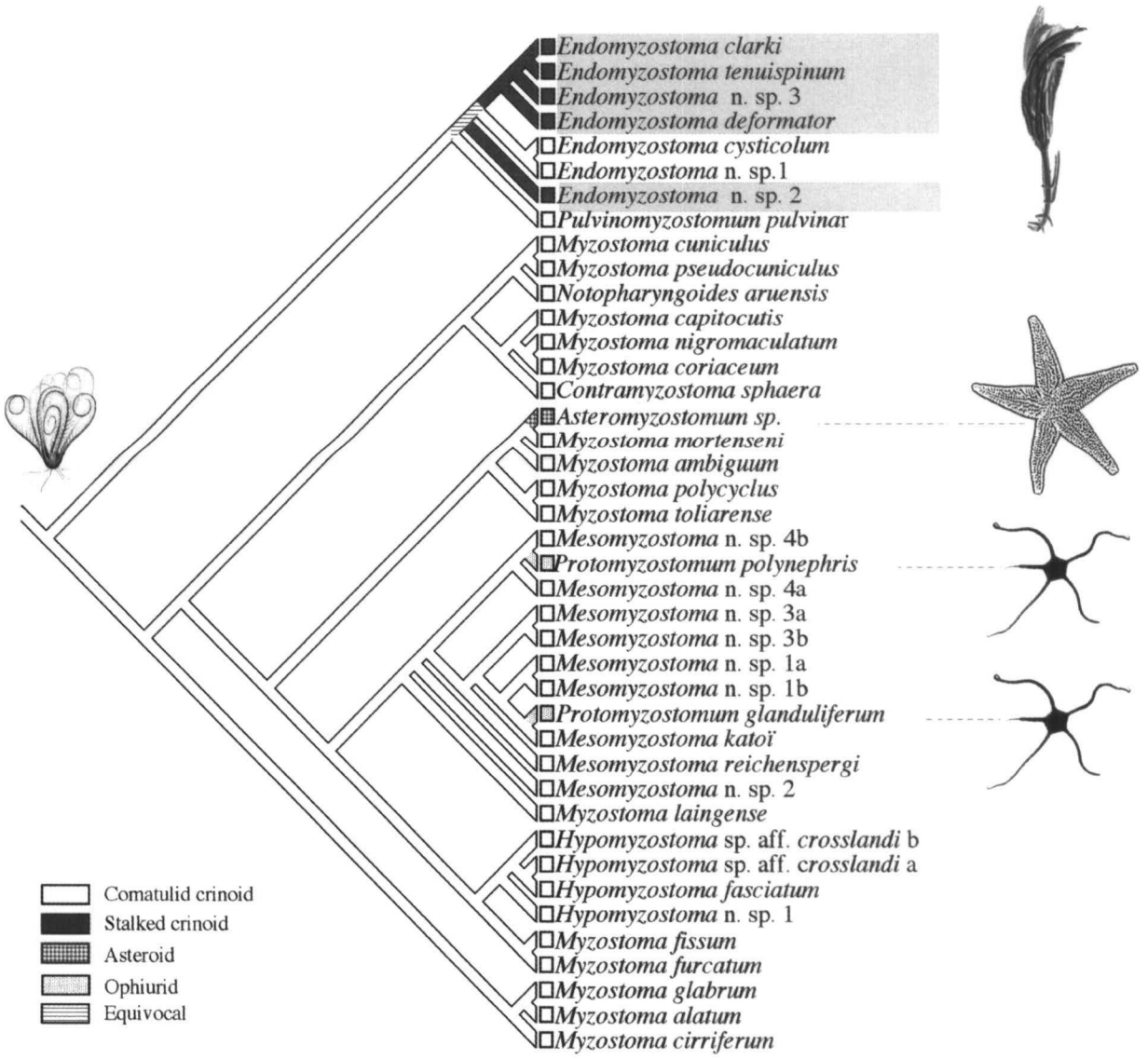

FIGURE 8. MP reconstruction of the evolution of myzostomid host's preferences. Grey boxes indicate association with stalked crinoids while all other species are associated with comatulid crinoids. Dotted lines indicate association with a non-crinoid host (note that the phylogenetic position of these three myzostomids have been estimated only from 18S rDNA data; cf. Table 4 and Fig. 6).

Protomyzostomum species (see Fig. 6), and (ii) the division of the polyphyletic *Myzostoma* into various new monophyletic genera.

Mapping of ecological characters on our molecular phylogenies suggests that the ancestors of myzostomids infested comatulid crinoids, then one of its descendent lineages shifted toward association with stalked crinoids while shifts towards infestation of asteroids and ophiuroids occurred several times independently. Hence, the deformities observed on fossilized stalked crinoids of the Late Ordovician (around 435 million years ago; Warn, 1974) and of the Carboniferous might not have been induced by myzostomids because comatulid crinoids first appeared in the Jurassic era (around 144 million years ago; Ubaghs, 1978). Some marks on stalked crinoid fossils dating from Silurian (around 412 million years ago), however, are very similar to galls induced by extant myzostomids: they are close to ambulacral grooves, made of host's ossicles, and have two openings (Brett, 1978). These openings allow myzostomids to catch food particles from crinoid ambulacral grooves and to expulse faeces from their shelters (Eeckhaut and Jangoux, 1995). Obviously, the inference of ancestral character states should be considered with caution as an ancestral association with stalked crinoids requires a single additional shift. Furthermore, the massive extinction of stalked crinoids at the end of the Permian period (around 248 million years ago) might have caused the coextinction of several basal lineages of myzostomids, hence, possibly biasing our inference of ancestral host association (see Omland, 1999).

Although MP reconstruction analysis of the myzostomid ancestor lifestyle is ambiguous (parasite of the digestive system, or gallicolous, or ectocommensal), ML

inference suggests that the basal myzostomid was an ectocommensal. This result would reinforce the general observation that there is, in Metazoa, no published evidence of free-living or ectocommensal organisms that evolved from parasites. However, it is noteworthy that in the few ectocommensal *Myzostoma* species for which the ontogeny is known (e.g., *M. cirriferum* and *Myzostoma* sp.; Eeckhaut and Jangoux, 1993, and Kato, 1952, respectively), the life cycle includes (i) a free-living pelagic larval stage that (ii) metamorphoses into a juvenile stage attaching for a few months by its chaetae on the crinoid integument, and finally (iii) a mobile ectocommensal adult stage (Eeckhaut and Jangoux, 1993). The first post-metamorphic stage in ectocommensal myzostomids is thus a parasitic stage during which the myzostomid induces deformities to the host's epidermis and dermis (Eeckhaut and Jangoux, 1993). It is therefore plausible that the first myzostomids fixed firmly to crinoids with their chaetae and induced the formation of galls that would protect them from predation.

The ancestral lineage of myzostomids probably split early into two lineages characterized mainly by gallicolous parasites and ectocommensals, respectively (Figs. 7A and 9). Males and females of most extant gallicolous myzostomids (as well as *P. pulvinar*) have marked sexual dimorphism. It is generally thought that these species are protandrous hermaphrodites (Grygier, 2000), with males being able to differentiate into females. A single male and a single female are often associated inside the gall (or in the digestive system for *P. pulvinar*). Females are large and cannot leave the gall or the digestive system of their crinoid host but males are much smaller (often classed as dwarf males) and can probably move easily on females (Eeckhaut and Améziane-Cominardi, 1994). In *Endomyzostoma* spp., the males certainly can leave galls and move at the surface of crinoids as they are smaller than the gall openings. It is probably at the male stage that lifestyle shifts (towards cysticolous parasitism, or back to ectocommensalism) occurred (Fig. 9).

The second major primary lineage (ectocommensals) of myzostomids gave rise to an array of diverse lifestyles: various ectocommensals (mobile or associated with arms or pinnules), ectoparasites, digestive system parasites, cysticolous parasites, and celom parasites (Fig. 9). Our analyses suggest that infestation of coelomic cavities (*Mesomyzostoma+Protomyzostomum*) evolved from arm ectocommensals (Fig. 7A). When considering the full phylogeny of myzostomids, each lifestyle, except parasitism of celomic cavities and gallicolous, evolved at least twice independently and from various ancestral states: e.g., the cysticolous *M. toliarense* and *C. sphaera* evolved from ectocommensals, whereas *E. cysticolum*, and*Endomyzostoma* n. sp. 1 evolved from gallicolous myzostomids.

Parasitism appeared multiple times during the evolution of Metazoa: within Protostomia, 40% of Ecdysozoa and 20% of Lophotrochozoa are parasites (De Meeus and Renaud, 2002). In the latter group, to which myzostomids

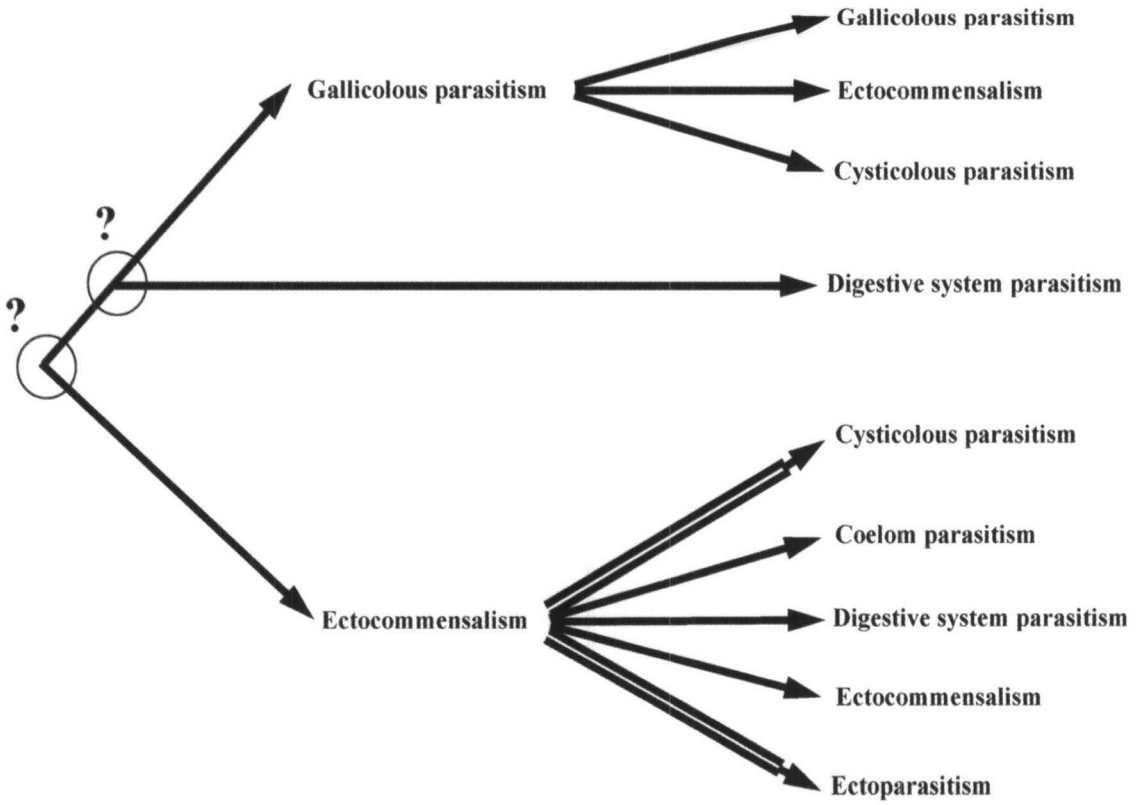

FIGURE 9. Schematic reconstruction of the evolution of the symbiotic lifestyles in myzostomids as suggested by the present phylogenetic analysis. Double arrows indicate multiple independent emergences.

belong, the highest number of parasites is found in Acantocephala (100%) and Platyhelminthes (79%), whereas only 7% of Annelida are parasites (De Meeus and Renaud, 2002). As in myzostomids, the nature of symbiosis is very diverse in Platyhelminthes: ectoparasitism is observed in Monogenea, and endoparasitism of various body parts of a wide range of host taxa characterizes Neodermata (i.e., the clade including Trematoda and Cestoda). Baguñà and Riutort (2004) suggest that ectoparasitism is the plesiomorphic condition within the group Monogenea + Neodermata, endoparasitism appearing once later on within the lineage that gave rise to extant trematodes and cestodes. On the other hand, phylogenetic analyses of 18S rDNA strongly suggest that parasitism in Nematoda evolved at least six times independently (Dorris et al., 1999).

ACKNOWLEDGMENTS

Comments from three anonymous reviewers allowed us to significantly improve the manuscript. Tatsuo Oji (University of Tokyo) provided Japanese specimens of myzostomids, Alexander Tzetlin (Moscow State University) provided *Protomyzostomum polynephris* specimens, Ilse Bartsch (Flanders Marine Institute; Alfred Wegener Institut für Polar- und Meeresforschung) provided the *Protomyzostomum glanduliferum* specimens, Kristian Fauchald (National Museum of Natural History Smithsonian Institution, Washington) provided the *Asteromyzostomum* sp. specimens, Nadia Ameziane-Cominardi (Musée d'histoires naturelles de Paris) provided the New Caledonian specimens, and Dr. Rich Mooi (California Academy of Natural Sciences) for the Antarctic crinoids. We are indebted to Dr. Charles Messing (Nova Southeastern University) for helping us in determining crinoid hosts. Thanks are also expressed to Daniel Monteyne, Patrick Mardulyn, and Sabrina Rosa (Laboratory of Evolutionary Genetics, Free University of Brussels, ULB) for their help and advice in sequencing. The National Fund for Scientific Research, Belgium (FRFC contract numbers 2.4.567.04.F and 2.4583.05), the "Fondation Agathon De Potter" (Académie Royale des Sciences, des Lettres et des Beaux-Arts de Belgique), and the "Communauté Française de Belgique" (ARC 12543/20022772) provided substantial support for this work. Déborah Lanterbecq is supported by a Ph.D. grant from the "Fonds pour la formation à la recherche dans l'industrie et dans l'agriculture" (FRIA). Greg Rouse was supported by the Australian Research Council and South Australian Museum.

REFERENCES

Baguñà, J., and M. Riutort. 2004. Molecular phylogeny of the Platyhelminthes. Can. J. Zool. 82:168–193.

Bremer, K. 1994. Branch support and tree stability. Cladistics 10:295–304.

Brett, C. E. 1978. Host-specific pit-forming epizoans on Silurian crinoids. Lethaia 11:217–232.

Crisp, M. D., and L. G. Cook. 2005. Do early branching lineages signify ancestral traits? Trends Ecol. Evol. 20:122–128.

Cunningham, C. W. 1997. Can three incongruence tests predict when data should be combined? Mol. Biol. Evol. 14:733–740.

Cunningham, C. W., K. E. Omland, and T. H. Oakley. 1998. Reconstructing ancestral character states: A critical reappraisal. Trends Ecol. Evol. 13:361–366.

De Meeus, T., and F. Renaud. 2002. Parasites within the new phylogeny of eukaryotes. Trends Parasitol. 18:247–225.

Dorris, M., P. De Ley, and M. Blaxter. 1999. Molecular analysis of nematode diversity. Parasitol. Today 15:188–193.

Eeckhaut, I. 1998. Mycomyzostoma calcidicola gen. nov., sp. nov., the first extant parasitic myzostome infesting crinoid stalks, with a nomenclatural appendix by M.J. Grygier. Species Diversity 3:89–103.

Eeckhaut, I., and N. Améziane-Cominardi. 1994. Structural description of three myzostomes parasites of crinoids and of the skeletal deformities they induce on their hosts. Pages 203–209 in Echinoderms through time. Proceedings of the Eight International Echinoderm Conference (B. David, A. Guille, J.-P. Feral, and M. Roux, eds.). A. A. Balkema, Rotterdam.

Eeckhaut, I., M. J. Grygier, and D. Deheyn. 1998. Myzostomes from Papua New Guinea, with related Indo-West Pacific distribution records and description of five new species. Bull. Mar. Sci. 62:841–886.

Eeckhaut, I., and M. Jangoux. 1991. Fine structure of the spermatophore and intradermic penetration of sperm cells in Myzostoma cirriferum (Annelida, Myzostomida). Zoomorphology 111:49–58.

Eeckhaut, I., and M. Jangoux. 1993. Life cycle and mode of infestation of Myzostoma cirriferum (Annelida), a symbiotic myzostomid of the comatulid crinoid Antedon bifida (Echinodermata). Dis. Aquatic Organ. 15:207–217.

Eeckhaut, I., and M. Jangoux. 1995. *Contramyzostoma bialatum* (Annelida: Myzostomida), a new genus and species of parasitic myzostome infesting comatulid crinoids. Raffles Bull. Zool. 43:343–353.

Eeckhaut, I., and D. Lanterbecq. 2005. Myzostomida: A review of their ultrastructure and phylogeny, in Morphology, molecules and evolution of the Polychaeta and related taxa. (T. Bartholomaeus, and G. Purschke, eds.). Hydrobiologia 535/536:253–275.

Eeckhaut, I., D. McHugh, P. Mardulyn, R. Tiedemann, D. Monteyne, M. Jangoux, and M. C. Milinkovitch. 2000. Myzostomida: A link between trochozoans and flatworms?. Proc. R. Soc. Lond. B 267:1–10.

Faith, D. P. 1991 Cladistic permutation tests for monophyly and nonmonophyly. Syst. Zool. 40:366–375.

Faith, D. P., and J. W. H. Trueman. 1996. When the topologydependent permutation test (T-PTP) for monophyly returns significant support for monophyly, should that be equated with (a) rejecting a null hypothesis of nonmonophyly, (b) rejecting a null hypothesis of 'no structure', (c) failing to falsify a hypothesis of monophyly, or (d) none of the above? Syst. Biol. 45:580–586.

Farris, J. S., M. Källersjo, A. G. Kluge, AND C. Bult. 1994. Testing significance of incongruence. Cladistics 10:315–319.

Felsenstein, J. 1985. Phylogenies and the comparative method. Am. Nat. 125:1–15.

Folmer, O., M. Black, W. Hoeh, R. Lutz, and R. Vrijenhoek. 1994. DNA primers for amplification of mitochondrial cytochrome c oxidase subunit I from diverse metazoan invertebrates. Mol. Mar. Biol. Biotech. 3:294–299.

Garey, J. R., T. J. Near, M. R. Nonnemacher, and S. A. Nadler. 1996. Molecular evidence for Acanthocephala as a subtaxon of Rotifera. J. Mol. Evol. 43:287–292.

Garey, J. R., A. Schmidt-Rhaesa, T. J. Near, and S. A. Nadler. 1998. The evolutionary relationships of rotifers and acanthocephalans. Hydrobiologia 387–388:83–91.

Gatesy, J., R. Desalle, and W. Wheeler. 1993. Alignment-ambiguous nucleotide sites and the exclusion of systematic data. Mol. Phylogenet. Evol. 2:152–157.

Gilbert, D. G. 1996. SeqPup version 0.6. Published electronically on the Internet, available via anonymous ftp to ftp.bio.indiana.edu.

Goloboff, P. A. 1993. Estimating character weights during tree search. Cladistics 9:83–91.

Grygier, M. J. 2000. Class Myzostomida. Pages 297–330 *in* Polychaetes and Allies: The Southern Synthesis. Fauna of Australia, Vol. 4A, Polychaeta, Myzostomida, Pogonophora, Echiura, Sipuncula (P. L. Beesley, G. J. B. Ross, and C. J. Glasby, eds.). CSIRO Publishing, Melbourne.

Hasegawa, M., K. Kishino, and T. Yano. 1985. Dating the human-ape splitting by a molecular clock of mitochondrial DNA. J. Mol. Evol. 22:160–174.

Huelsenbeck, J. P., B. Larger, R. E. Miller, and F. Ronquist. 2002. Potential applications and pitfalls of Bayesian inference of phylogeny. Syst. Biol. 51:673–688.

Jägersten, G. 1940. Zur Kenntnis der Morphologie, Entwicklung und Taxonomie der Myzostomida. Nova Acta Reg. Soc. Sci. Ups. (4) 11:1–84.

Jangoux, M. 1990. Diseases of Echinodermata. Pages 439–467 *in* Diseases of marine animals (O. Kinne ed.). Hamburg, Germany: Biologische Anstalt Helgoland.

Kato, K. 1952. On the development of myzostomes. ScienceReports of Saitama University, Series B (Biology and Earth Sciences) 1:1–16, plates I–III.
Kishino, H., and M. Hasegawa. 1989. Evaluation of the maximum likelihood estimate of the evolutionary tree topologies from DNA sequence data, and the branching order in Hominoidea. J. Mol. Evol. 29:170–179.
Lemmon, A. R., and M. C. Milinkovitch. 2002. MetaPIGA (Phylogeny Inference using the MetaGA) version 1.0.2b. Distributed by the authors (http:www.ulb.ac.be/sciences/ueg).
Lewis, P. O. 2001. A likelihood approach to estimating phylogeny from discrete morphological character data. Syst. Biol. 50:913–925.
Löytynoja, A., and M. C. Milinkovitch. 2003. A hidden Markov model for progressive multiple alignment. Bioinformatics 19:1505–1513.
Maddison, W. P., and D. R. Maddison. 2000. MacClade Version 4.0. Sinauer, Sunderland, Massachusetts.
Maddison, W. P., and D. R. Maddison. 2004. Mesquite: A modular system for evolutionary analysis. Version 1.01, http://mesquiteproject.org.
McHugh, D. 1997. Molecular evidence that echiurans and pogonophorans are derived annelids. Proc. Natl. Acad. Sci. USA. 94:8006–8009.
Messing, C. G. 1997. Living comatulids. Pages 3–30 *in* Geobiology of echinoderms (J. A. Waters and C. G. Maples eds.). Paleontological Society, London.
Meyer, D. L., and W. I. Ausich.1983. Biotic interactions among recent and among fossil crinoids. Pages 377–427 *in* Biotic interactions in recent and fossil benthic communities (Tevesz, M. J. S. and P. L. Mc Gall, eds.). Plenum Press, New York.
Nylander, J. A. A. 2002. MrModelTest, version 1.1b. Available from the authors at: http://www.ebc.uu.se/systzoo/staff/nylander.html.
Omland, K. E. 1999. The Assumptions and challenges of ancestral state reconstructions. Syst. Biol. 48:604–611.
Pagel, M. 1999. The maximum likelihood approach to reconstructing ancestral character states of discrete characters on phylogenies. Syst. Biol. 48:612–622.
Palumbi, S. R. 1997. Nucleic acids II: The polymerase chain reaction. Pages 205–247 *in* Molecular systematics, 2nd edition (D. M. Hillis, C. Moritz, and B. K. Mable, eds). Sinauer Associates, Sunderland, Massachusetts.
Posada, D., and K. A. Crandall. 1998. ModelTest: Testing the model of DNA substitution. Bioinformatics 14:817–818.
Ronquist, F. 2004. Bayesian inference of character evolution. Trends Ecol. Evol. 19:475–481.
Ronquist, F., and J. P. Huelsenbeck. 2003. MrBayes 3: Bayesian phylogenetic inference under mixed models. Bioinformatics 19:1572–1574.
Rouse, G. W., and K. Fauchald. 1997. Cladistics and polychaetes. Zool. Scripta 26:139–204.
Roux, M., C. G. Messing, and N. Ameziane. 2002. Artificial keys to the genera of living stalked crinoids (Echinodermata). Bull. Mar. Sci. 70:799–830.
Sambrook, J., E. F. Fritsch, and T. Maniatis. 1989. Molecular cloning. A laboratory manual. Cold Spring Harbor Laboratory Press, Cold Spring Harbor, New York.
Shimodaira, H., and M. Hasegawa. 1999. Multiple comparisons of log-likelihoods with applications to phylogenetic inference. Mol. Biol. Evol. 16:1114–1234.
Stummer-Traunfels, R. R. von. 1903. Beiträge zur Anatomie und Histologie der Myzostomem. I. Myzostoma asteriae Marenz. Zeitschrift für wissenschaftliche Zoologie 85:495–595.
Swofford, D. 1998. PAUP*: Phylogenetic analysis using parsimony (*and other methods). Beta version 4.0.b1, Sinauer Associates, Sunderland, Massachusetts.
Thompson, J. D., T. J. Gibson, F. Plewniak, F. Jeanmougin, and D. G. Higgins. 1997. The CLUSTAL X windows interface: Flexible strategies for multiple sequence alignment aided by quality analysis tools. Nucleic Acids Res. 24:4876–4882.
Ubaghs, G. 1978. Classification of the echinoderms. in Treatise on invertebrate paleontology (T) 2(1).
Van De Peer, Y., E. Robbrecht, S. Dehoog, A. Caers, P. De Rijk, and R. De Wachter. 1998. Database on the structure of small subunit ribosomal RNA. Nucl. Acids Res. 27:179–183.
Warn, J. M. 1974. Presumed myzostomid infestation of an ordovician crinoid. J. Paleontol. 48:506–513.
Wheeler, W. M. 1905. A new Myzostoma parasitic in starfish. Biol. Bull. 8:75–78.
Zrzavy, J., V. Hypsa, and D. F. Tietz. 2001. Myzostomida are not Annelids: Molecular and morphological support for a clade of animals with anterior sperm flagella. Cladistics 17:170-198.
Zrzavy, J., S. Mihulka, P. Kepka, A. Bezdek, and D. Tietz. 1998. Phylogeny of the metazoa based on morphological and 18S ribosomal DNA evidence. Cladistics 14:249–285.

First submitted 5 August 2004; reviews returned 23 November 2004; final acceptance 1 September 2005
Associate Editor: Marshal Hedin

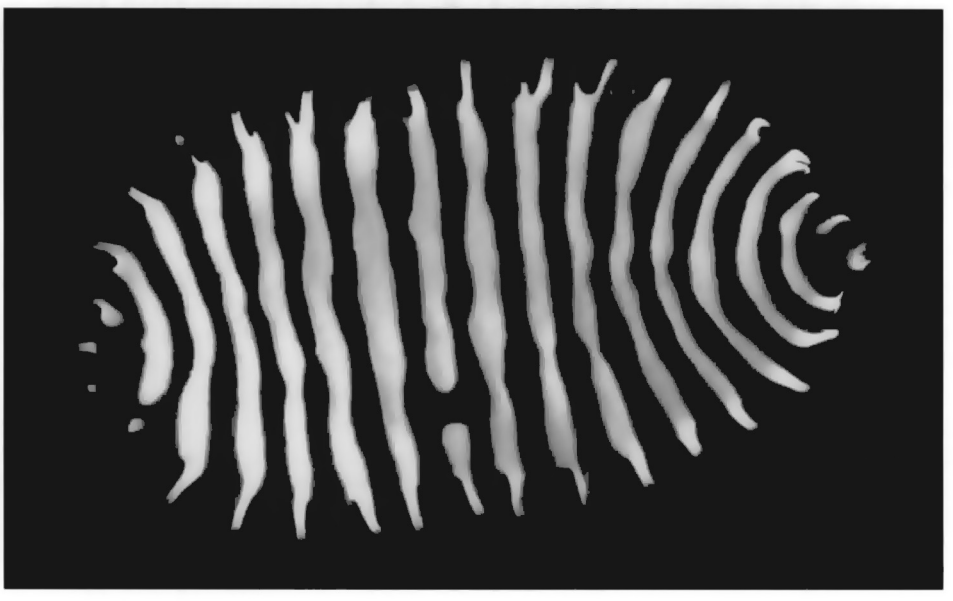

Light micrograph of *Hypomyzostoma dodecephalcis* (Grygier, 1992), an ectocommensal myzostomid living on the arms of the featherstar crinoid *Zygometra elegans* from the Great Barrier Reef.